



A11103 692961

REFERENCE

NIST
PUBLICATIONS**NISTIR 4751**

**Summary Report of NIST's
Industry-Government
Consortium Research
Program on Flowmeter
Installation Effects
With Emphasis on the
Research Period
May 1989 - February 1990:
Tube Bundle Effects**

**G. E. Mattingly
T. T. Yeh**

U.S. DEPARTMENT OF COMMERCE
Technology Administration
National Institute of Standards
and Technology
Chemical Science and Technology
Laboratory
Process Measurements Division
Fluid Flow Group
Gaithersburg, MD 20899

U.S. DEPARTMENT OF COMMERCE
Rockwell A. Schnabel, Acting Secretary
NATIONAL INSTITUTE OF STANDARDS
AND TECHNOLOGY
John W. Lyons, Director

QC

100

.U56

#4751

1991

NIST

NATIONAL INSTITUTE OF STANDARDS &
TECHNOLOGY
Research Information Center
Gaithersburg, MD 20899

**Summary Report of NIST's
Industry-Government
Consortium Research
Program on Flowmeter
Installation Effects
With Emphasis on the
Research Period
May 1989 - February 1990:
Tube Bundle Effects**

**G. E. Mattingly
T. T. Yeh**

U.S. DEPARTMENT OF COMMERCE
Technology Administration
National Institute of Standards
and Technology
Chemical Science and Technology
Laboratory
Process Measurements Division
Fluid Flow Group
Gaithersburg, MD 20899

November 1990

Issued December 1991



**U.S. DEPARTMENT OF COMMERCE
Rockwell A. Schnabel, Acting Secretary
NATIONAL INSTITUTE OF STANDARDS
AND TECHNOLOGY
John W. Lyons, Director**

PREFACE

The research results reported in this document were produced with the support of a National Institute of Standards and Technology (NIST) initiated industry-government consortium. In this mode of operation, there is a high degree of interaction between the representatives of the consortium member companies and the NIST researchers. Their interactions include: (1) the planning of the specific focus of the NIST research efforts, (2) the analyses of the results obtained, and (3) the conclusions drawn for the particular phase of the work. For this reason, it is pertinent to acknowledge both the support given to this phase of the research program and the technical contributions made by the representative of the consortium members.

The current consortium as of February 1990 is, alphabetically:

1. Ametek-McCrometer
2. Chevron Oil
3. Controlotron
4. Dow Chemical Co.
5. E.I. Dupont de Nemours
6. Ford Motor Co.
7. Gas Research Institute*
8. Gas Unie (The Netherlands)
9. Instrument Testing Service
10. ITT Barton
11. Kimmon Mfg. Ltd. (Japan)
12. NIST-Boulder
13. Rockwell International
14. Rosemount

*Specific acknowledgement is due to Dr. Kiran M. Kothari of the Gas Research Institute (GRI). Both his support of this program and his technical inputs in the analyses of results and in the conclusions drawn are gratefully acknowledged.

TABLE OF CONTENTS

	<u>Page</u>
PREFACE.....	iii
ABSTRACT.....	1
INTRODUCTION.....	1
VELOCITY PROFILE MEASUREMENTS.....	2
EFFECTS ON FLOWMETERS	
1. Orifice-Type Flow Meter.....	5
2. Turbine Meter.....	6
CONCLUSIONS.....	7
REFERENCES.....	8

Summary Report of NIST's Industry-Government Consortium Research
Program on Flowmeter Installation Effects
with Emphasis on the Research Period
May 1989 - February 1990: Tube Bundle Effects

G.E. Mattingly
T.T. Yeh

Fluid Flow Group
Process Measurements Division
Chemical Science and Technology Laboratory
National Institute of Standards and Technology
Gaithersburg, Maryland 20899

ABSTRACT

This report presents results produced in a consortium-sponsored research program on flowmeter installation effects. This project is a collaborative one that has been underway for four years; it is supported by an industry-government consortium that meets twice yearly to review and discuss results and to plan subsequent phases of the work. This report contains the results and conclusions of the recent meeting of this consortium at NIST-Gaithersburg, MD in February 1990.

The objective of this research program is to produce improved flowmeter performance when meters are installed in non-ideal conditions. This objective is being attained via a strategy to (a) measure, understand, and quantify the salient features of non-ideal pipe flows from such pipeline elements as elbows, reducers, valves, flow conditioners, etc. or combinations of these, (b) correlate meter-factor shifts for selected types of flowmeters, relative to the features of these non-ideal pipe flows so as to be able to predict meter performance accurately in non-ideal installations, and (c) disseminate the resulting technology through appropriate channels such as publishing our results in pertinent journals and upgrading paper standards for flow measurements.

Specific results included in this report for the pipe flow from single and double elbow out of plane configurations followed by a conventional 19-tube, concentric tube bundle are:

1. the distributions of the mean and the turbulence velocities in the axial and vertical directions both up- and downstream of the tube bundle, and
2. the performance of orifice and turbine flowmeters installed downstream of these elbows and tube bundle arrangement.

INTRODUCTION

The increasing scarcity of fluid resources and the rising value of fluid products are placing new emphases on improved measurements. Improvements are sought from many starting points. Meters are being retrofitted into fluid systems that were not designed for them. This invariably means the flowmeters are being inserted in non-ideal installation conditions. Increased accuracy levels are desired for installed meter systems - either by upgrading the flow conditions that enter the meter or by replacing the device itself and/or its auxiliary components.

Flow conditioning devices of one geometry or another are frequently recommended in metering standards for improving flowmeter performance when installation conditions are not ideal. However, the pipeflows generated by these devices have to be considered in terms of the flowmeter installed downstream and the pertinent parameters that control pipeflow phenomena and that influence the performance of the particular meter. It will be shown in what follows that certain flow conditioner installations can produce serious deviations from the performance of specific meters in ideal installation conditions.

The industry-government consortium research program on flowmeter installation effects that is currently underway at NIST is designed to help improve fluid metering performance when installation conditions are not ideal. The design of the program is to produce a basic understanding of the flow phenomena that are produced in non-ideal pipe flows and to quantify these phenomena. When these phenomena and their quantified characteristics are correlated with the performance of specific types of meters, it should be feasible to predict and achieve satisfactory measurements in non-ideal meter installations. The success of this approach has been demonstrated using several different types of flowmeters installed downstream of several different pipe elbow configurations.

The experimental research program is based upon the measurements of pipe flows from selected piping configurations using laser Doppler velocimetry (LDV). [1-4] Selections of piping configurations and pipeline elements such as flow conditioners are done by vote of the consortium members; one or two such configurations can be done in one year.

The LDV techniques that have been and are being applied to determine pipe flows can also be used to measure the effects of other pipeline elements - valves, flow conditioning elements (for fluid velocity or pulsations, etc.), mixing devices, generic flowmeter geometries - or combinations of these. The resulting understanding provides the basis for improving the effectiveness of these devices and, in turn, the performances of flowmeters installed downstream and, thus, for increasing the productivity of the continuous processes which depend upon them. [4-8]

In the present study, the fluid is water and the piping is 52.5 mm diameter (2 in.), smooth, stainless steel. The relative roughness of this pipe has been measured with a profilometer to indicate a value of 0.006%. Diametral Reynolds numbers range up to 10^5 . According to the concepts of dynamic similitude, the results of the present research program should predict a range of other flows - both liquids and gases - when pertinent parameters match those in our experiments.

When the performance of flowmeters - similar to or different from those selected - is determined by calibration tests, meter performance can be correlated to pipe flow parameters. When this is achieved - by flowmeter manufacturers or users alike - it should then be possible to predict satisfactory metering performance for these meters in similar non-ideal installations.

VELOCITY PROFILE MEASUREMENTS

In what follows, results are presented for the pipe flow effects produced by installing a conventional, tube-bundle type flow conditioner downstream of two different pipe configurations. The first configuration is the single, long-radius elbow which produces a secondary flow pattern that has two counter-rotating vortices on either side of the center plane of the elbow. The second configuration is the double elbow out-of-plane configuration where the elbows are connected with no straight pipe length between the elbows. This configuration produces a complicated, single vortex secondary flow pattern that persists for considerable distances in the downstream piping. These distances greatly exceed those for the single elbow.

The two elbow configurations investigated are sketched in figure 1. In figure 1(a) the single elbow arrangement is shown with the coordinate system. This single elbow was oriented to turn a vertically downward pipe-flow into the horizontal piping where the LDV measurements were made. The coordinate system has its origin on the pipe centerline in the exit plane of the long radius elbow. This elbow has a centerline-radius of curvature of $3 D/2$, where D is the pipe diameter. The velocity components in the Y and Z directions are designated V and

*Square bracketed integers refer to references given below.

W, respectively. No measurements were made of the U component in the X direction. The Reynolds numbers investigated were 10^4 and 10^5 based on pipe diameter. At the right side of figure 1(a) is sketched the dual vortex secondary flows as they might appear looking upstream. The designation "L-Y" is intended to denote that "L" is the configuration consisting of a long radius elbow into which a pipeflow enters from the "-Y" direction.

In figure 1(b) is sketched the basic double elbow out-of-plane configuration. The coordinate system is oriented in the exit plane of the second elbow as described above. The designation "L+X-Ys" is intended to denote that both elbows are of the long radius type. The "+X" is to show that the entering pipeflow is in this direction; the "-Ys" is to indicate that the first elbow turns the flow from the entering direction into the downward direction. The "s" is to indicate the diametral length of any pipelength that might be placed between the elbows. In the results presented here, no such pipelengths existed and therefore "s=0" indicates the two elbows were welded together. The second elbow turns the flow again into the Z direction. At the right in figure 1(b) is shown the rotational direction of the single vortex looking upstream. This vortex is not symmetrical about the pipe centerline. For details, see [1-4].

For the results described below, all lengths are non-dimensionalized using the inside pipe diameter; all velocities are non-dimensionalized using the bulk velocity, W_b . The roughness of the stainless steel pipe was measured using a profilometer. Average values of the roughnesses ranged from 3 to 5 μm (125 to 200 microinches); in nondimensionalized terms these values produced relative roughness values of 0.00006 to 0.0001. The glass pipe through which the LDV measurements were made gave roughness results from 0.1 to 0.2 μm (5-10 microinches) or, in relative roughness, 0.000005 to 0.00001.

The tube bundle installed in these pipeflows is shown in figure 2. This is a geometrically scaled version of the concentric-type tube bundle flow conditioner that is prevalently used in metering practice in the U.S. This tube bundle is approximately two diameters in length; it has a porosity of about 90%. The areas outside the tubes are not filled.

This tube bundle was installed in the downstream pipe as sketched in figure 3, where all dimensions are given in pipe diameters. This shows that the inlet of the tube bundle is 3.8 diameters from the exit plane of the upstream elbow. The length "C" is the distance, in diameters, downstream of the outlet plane of the tube bundle.

The measurements of the axial velocity profiles downstream of the single elbow, with the tube bundle installed as shown, are given for $Re = 10^5$ in figure 4. The designation "L-Y, FC1" is to indicate that the single elbow described above is followed by the tube bundle flow conditioner, installed as shown in figure 3.

These results show the profiles both upstream of the tube bundle and for a range of distances downstream as indicated for the values of Z given in the legend. The dashed line shown in the figure is the power law profile for these conditions.[5] The slope discontinuity resulting from the power law distribution at the pipe centerline has been removed by a smoothing technique. This technique consists of fitting a second order polynomial through velocity values at $\pm 5\%$ of the pipe diameter on either side of the pipe centerline and matching slopes at these points. The results in figure 4 show that the profile upstream of the tube bundle entrance at $Z = 2.7$ is essentially the same as that measured without the tube bundle, see [1-3]. The profile measured at $Z = 6.2$ just downstream of the tube bundle exit clearly shows the jetting effects produced by the individual flows through the tubes and through the spaces between tubes. It is also noted that the axial velocities adjacent to the pipe wall are quite high compared to the power law values in these regions. This seems to indicate that the high values of the axial velocity that flow from the elbow pass between the tube bundle and the pipe wall. However, with downstream distance, the viscous effects near the pipewall

reduce these high velocities to the values of the power law distribution by about the $Z = 20$ location. However, at the $Z = 19.2$ position; it is noted that the axial velocity in the core region near the pipe centerline remains about 10% of the bulk velocity slower than the power law values. This slowed-core region spans about 35% of the pipe diameter. At the $Z = 33.7$ position, it is found that the axial velocities in the center core region of the pipe flow have values which exceed those of the power law distribution. This region spans about 30% of the pipe diameter. From the description given above for the smoothing technique applied to remove the slope discontinuity of the power law profile in a very small region near the centerline, this technique is not producing the observed axial velocity overshoot in comparison to the power law values. It is recalled from earlier published results that the pipeflow from the single elbow for these $Re = 10^5$ conditions closely compares to the power law distribution.[3-4]

In figure 5 are plotted the streamwise component of the pipeflow velocity along the vertical diameter for $Re = 10^5$ for several downstream positions. The dashed line gives the power law profile as mentioned for figure 4. The most upstream profile is measured upstream of the tube bundle and shows significantly slowed flow over most of the center of pipe with a small region of fluid exceeding the speed of the power law profile and a larger region of high speed flow at the bottom of the pipe. The profile at $Z = 6.2$ shows the jetting effects produced by the flows from the individual tubes. Downstream of this location at $Z = 11.2$ these jetting effects are smoothed and the profile qualitatively resembles that measured upstream of the tube bundle. Downstream of this location at $Z = 19.2$ the measured distribution shows that the high speed flow at the bottom of the pipe is only slightly faster than that of the power law profile. At this location, there continues to be a slow core of fluid at and near the center of the pipe. At $Z = 33.7$, the profile shows good agreement with the power law distribution at the top and bottom of the pipe, and over a significant portion of the middle of the pipe the velocity is found to exceed the power law values.

The vertical velocity profile along the horizontal diameter for $Re=10^5$ is shown in figure 6. The profile at $Z=2.7$ shows the distribution produced by the counter-rotating vortices. Immediately downstream of the tube bundle, the profile is diminished significantly and at all successive locations, the vertical velocity is zero.

Figure 7 presents results for the vertical velocity profile along the vertical diameter for $Re=10^5$. The profile upstream of the tube bundle is the same as that measured without the tube bundle, see [1]. The profile just downstream of the tube bundle show that the tube bundle significantly reduces the vertical velocity and at successive locations, the vertical velocity is essentially zero across the pipe. Figures 6 and 7 show that the tube bundle effectively reduces the time averaged velocities which are normal to the pipe centerline.

The streamwise component of the turbulent velocity both upstream and downstream of the tube bundle is shown in root-mean-square (rms) form in figure 8 for $Re=10^5$. The dashed profile shows the distribution measured by Laufer, see [6]. At $Z=2.7$ the profile is the same as that measured without the tube bundle, see [2]. At $Z=6.2$, the turbulence level and distribution show the effects of the tube bundle. The peaks in this distribution reflect the interactions between the jetting flows from individual tubes. At successive locations, the distributions first change to the qualitative form of the Laufer results and then approach quantitative agreement with this profile. It is noted that the present results do not conform precisely to the Laufer results. This may be due to the different conditions which produced each flow.

Figure 9 presents the rms profiles for the vertical component of the turbulent velocity along the horizontal diameter for $Re=10^5$. The dashed line shows Laufer's results. Again, the profile upstream of the tube bundle is the same as that measured in the absence of the tube bundle, see [2]. Downstream of the tube bundle, the profile shows the effects of the interactions of the jetting flows

from individual tubes. Further downstream, the profile changes to qualitatively resemble the Laufer distribution while having a higher level. At $Z=33.7$, the profile agrees more closely with the Laufer distribution, but still lies above it.

Figures 10 through 15 present results analogous to these of figures 4-9 for $Re=10^4$. In each case the salient features parallel those observed for the $Re=10^5$ case.

Figure 16 presents the mean velocity profiles for the streamwise component of the pipeflows downstream of the closely coupled double elbows out of plane where the tube bundle is positioned as shown in figure 3. Because our previous single elbow results indicate that the tube bundle does not alter the profile one diameter upstream from it, the following double elbow results with the tube bundle are presented using measurements made at $Z = 2.6$ without the tube bundle. The profile denoted by the asterisk upstream of the tube bundle is that measured without it, see [1-3]. This convention holds for figures 16-27. The dashed line shows the power law profile for these conditions as described for figure 4. The profile at $Z=7.2$ which is 1 diameter downstream from the exit plane of the tube bundle does not exhibit the jetting flow effects noted in the corresponding figures 4 and 10 where results were measured at $Z=6.2$. It is also noted here that because of viscous wall effects, the high speed flows near the pipewall approach the power law values before the slower core flow in the center of the pipe. At $Z=33.7$ this core flow is noted to flow faster than the power law values.

In figure 17 are shown the axial velocity profiles versus position along the vertical diameter for different locations upstream and downstream of the tube bundle flow conditioner for $Re=10^5$. Again, it is noted that the profile upstream of the tube bundle is that measured without the tube bundle. The dashed profile is that for the power law for these conditions. It is again noted that at successive downstream locations the high speed layers near the pipewall more rapidly approach the power law values than does the slower core flow near the middle of the pipe. At $Z=34.6$, the velocity of the flow in the center core of the pipe is higher than the power law values. Again, it is noted that the radial extent of the region where the velocity exceeds that for the power law distribution is larger than that associated with the centerline smoothing procedure mentioned above, indicating that this procedure is not the cause of the "over developed" velocity profile. This "over development" could be either the result of the tube bundle effects on the pipeflow profile or due to the natural equilibration of pipe flows.

Figures 18 and 19 show the vertical velocity distribution both upstream and downstream of the tube bundle along horizontal and vertical diameters, respectively, for $Re=10^5$. As before, the distribution for the ideal pipeflow is zero everywhere. These results show that, at both downstream locations, the tube bundle has effectively reduced the vertical velocity to zero.

Figures 20 and 21 present results for the rms values of streamwise and vertical components of the turbulent velocity upstream and downstream of the tube bundle for $Re=10^5$. In both of these, the upstream results are not influenced by the presence of the tube bundle. Downstream of the tube bundle increased levels of turbulence are observed in the wakes of the tubes and these levels subside to approach, but do not reach, the Laufer levels.

Figures 22 through 27 present results for $Re=10^4$ that are analogous to those of figures 16-21. In each case, observations are similar to those above for this more viscous case.

EFFECTS ON FLOWMETERS

a. Orifice-Type Flow Meter. Figures 28(a) and (b) present calibration results for a flange-tapped orifice flowmeter having $\beta=0.5$ installed at different distances downstream of the double elbow out of plane configuration without and

with the tube bundle. The beta ratio is that of orifice hole to inside pipe diameter. The legend on each plot gives the downstream locations in terms of Z or C in diameters as defined in figure 3, where $Z=C+5.7$. The ordinate scale of each figure is the percentage change of the discharge coefficient relative to that for the $Z=210$ location at each flowrate. Therefore, the results for this $Z=210$ position and those near it show zero or values near zero. When this meter is installed near the exit plane of these elbows, the discharge coefficients are shifted to positive values as high as 2-3%. When the orifice meter is installed just downstream of the tube bundle, the shift is negative and of the same magnitude. The erratic nature of the shift in discharge coefficient for the position closest to the tube bundle is judged to be due to the high levels of turbulence produced by this tube bundle, see figures 20-21 and 26-27. As this meter is moved downstream of the tube bundle the negative shift in orifice discharge coefficient C_d diminishes to zero and then increases to positive levels of as much as +0.2%. With further downstream distance this positive shift is reduced to zero for positions between 40-50 diameters. Without the tube bundle, figure 28(a) shows that the "zero-shift" C_d position is approximately 90 diameters from this elbow configuration. It is therefore concluded that the installation of this tube bundle could save 40-50 diameters of upstream piping.

Figures 29(a) and (b) show summarized results for the effects of this tube bundle on a range of orifice meters installed downstream of this double elbows out-of-plane configuration. The ordinate scale for both figures is the mean discharge coefficient averaged over ranges of flowrate where turndowns are about 3. These flowrate ranges - in terms of Reynolds number - vary with beta ratio as follows: $\beta=0.363$, $1,500 \leq Re \leq 45,000$; $\beta=0.5$, $30,000 \leq Re \leq 75,000$; $\beta=0.75$, $45,000 \leq Re \leq 100,000$. The results in figure 29(a) show that the smaller beta meters are shifted positively by the flows produced by this elbow configuration. For the $\beta=0.75$ orifice the meter shift is negative for installations less than about 70 diameters downstream. The erratic nature of the data for installation near the tube bundle is undoubtedly due to the complicated, helical nature of the secondary flow produced by this elbow configuration. Beyond this $Z=75$ point, the shift is positive reaching a level of about +0.3% at $Z=90$ followed by a slow reduction toward zero that is estimated to occur at about the location $Z=150$. Figure 29(b) shows that the tube bundle markedly alters these results. When the tube bundle is installed as shown in figure 3, the shifts determined for all three beta installations near the tube bundle are negative. The magnitudes of these negative shifts increase with beta ratio. As the orifice is located further downstream of the tube bundle, these negative shifts decrease and pass through zero for $C=11-13$. Beyond this location the orifice shift is positive, attaining peak values that increase with beta ratios with a maximum of about +0.8% for $\beta = 0.75$. This level of positive shift occurs over a significant length of piping and for the specific conditions of the present experiments, this interval is quantified as $25 \leq C \leq 35$.

Beyond these locations, the shift diminishes to zero for differing downstream distances that again increase with beta ratio with a maximum of about $Z=135$ for the largest beta.

b. Turbine Meter. Figures 30(a) and (b) present, respectively, calibration data for the selected turbine-type flowmeter installed at various positions downstream of the double elbows-out-of-plane configuration without and with the tube bundle. The ordinate scale gives the percentage change of the Strouhal number

$$St = fD/W_b$$

at each flowrate relative to the value obtained for the very long ($Z=210$) installation condition. Without the tube bundle, this meter's Strouhal number, as shown in figure 30(a), is shifted up almost 2% by the flow effects from this elbow configuration when this meter is installed close to it. This shift is still

evident even at the $Z=135.8$ downstream position. When the tube bundle is installed between these elbows and this meter, the previously noted positive shifts are markedly reduced as shown in figure 30(b), although not to zero even within 20 diameters downstream where the mean shift over the flowrate range tested is more than 0.1%. It is also noted from figure 30(b) that the shift phenomena for this meter is not monotonic in C . This pattern is shown in figure 30(c); this figure includes the shift distribution without the tube bundle. It is recalled that figures 18 and 24 show that the time averaged swirl distributions along the horizontal diameter are essentially zero downstream of the tube bundle. Therefore, it appears that this meter has its meter factor shifted positively through the mean velocity profile distortions or the turbulent flow developments produced by this tube bundle. It is also concluded from the results shown in figure 30(c) that the shift in meter factor for this meter in these conditions can be reduced to below $\pm 0.1\%$ for the position $Z=42$ or $C=36$ using this tube bundle.

CONCLUSIONS

Based upon our laser velocity surveys it is concluded that for both the single elbow and the tube bundle and the closely coupled double elbow out of plane configuration and the tube bundle:

1. The tube bundle does significantly change both the mean and the turbulent velocity distributions measured downstream of it and these deviations diminish with distance,
2. The tube bundle does significantly reduce swirl to very low levels through the effects of the tubes on the azimuthal and radial components of the mean pipeflow. The tube bundle produces pronounced jetting effects due to the flows out of the individual tubes.
3. The interactions between the jetting flows from adjacent tubes appears to generate high levels of turbulence,
4. The distributions of both mean and turbulent velocities result from the non-uniform porosity of this tube bundle arrangement,
5. The mean axial profile "over-develops" in the downstream piping some 35 diameters from the tube bundle. This result occurs for $Re = 10,000$ and $100,000$.

The tube-bundle-conditioned flows from the double elbow configuration appear to perturb significantly the performance of several types of flowmeter - i.e., orifice and turbine. Specific conclusions are:

1. The orifice discharge coefficients for all beta ratios tested are reduced relative to reference values when these meters are installed within about fifteen (15) diameters from the exit plane of the tube bundle. The reductions are dependent on beta ratios; larger reductions occur for larger beta ratio. When these meters are installed seven (7) diameters downstream of the tube bundle, the reductions range to -2.5% of the reference value.
2. For orifice installation positions from about fifteen (15) diameters to about fifty (50) diameters or more, the discharge coefficients are found to be shifted above the reference values. These shifts are largest for the largest beta ratio and range to +0.8% of the reference value.
3. These orifice discharge coefficient shift results closely resemble those previously determined for installations downstream of the single elbow and tube bundle. As both of these results closely resemble orifice shifts produced by other investigators for installation in straight piping, it is concluded that the effects of the tube bundle appear to be the dominant factor influencing the performance of orifice meters installed downstream.

4. The orifice discharge coefficient shifts which are negative relative to reference values when the meter is installed near the exit plane of the tube bundle is interpreted to be due to the uniformity of the mean axial velocity profile in this region. This uniformity causes enhanced pressure levels to be present at the upstream tap location (relative to reference values) and this produces lowered discharge coefficients.
5. The positive orifice discharge coefficient shifts determined for installation positions greater than fifteen (15) diameters downstream of the tube bundle are interpreted to be due to the "over-development" of the center core of the mean axial velocity profile in this region. This overdevelopment produces reduced levels of pressure in the region of the upstream orifice tap thus reducing the differential pressure and thereby increasing the discharge coefficient.
6. The marked overdevelopment of the central core of the mean axial velocity profile could be a result of the enhanced turbulence put into the pipeflow by the tube bundle geometry or it could be natural pipeflow development under these conditions.
7. The tube bundle effects on the performance of this specific turbine meter when it is installed downstream of the closely coupled double elbow-out-of-plane reduce the high positive shifts observed without the tube bundle. These shifts which reach almost 2.0% without the tube bundle were lowered to 0.2% or less with the tube bundle. While the meter factor of this meter was shifted +0.2% when it was installed 125 diameters downstream of the double elbows out of plane configuration, it was also found to be only shifted 0.1% or more when installed between 10 and 40 diameters downstream of this double elbow configuration and tube bundle arrangement.

REFERENCES

1. Mattingly, G.E. and Yeh, T.T., NIST's Industry-Government Consortium Research Program on Flowmeter Installation Effects: Report of Results for the Research Period Nov. 1988 - May 1989, NISTIR 4310, Apr. 1990.
2. Mattingly, G.E. and Yeh, T.T., NIST's Industry-Government Consortium Research Program on Flowmeter Installation Effects: Report of Results for the Research Period June - December 1987. NISTIR-88-3898, May 1988.
3. Mattingly, G.E., and Yeh, T.T., NIST's Industry-Government Consortium Research Program on Flowmeter Installation Effects: Report of Results for the Research Period Jan. - July 1988, NISTIR-89-4080, Apr. 1989.
4. Mattingly, G.E., Yeh, T.T., Robertson, B. and Kothari, K., NBS Research on In-Situ Flowmeter Installations, Procs, AGA Distribution and Transmission Confr. Las Vegas NV, May 1987.
5. Schlichting, H., Boundary Layer Theory, McGraw-Hill Book Co., 6th edition, New York, 1968.
6. Laufer, J., The Structure of Turbulence in Fully Developed Pipe Flow, NBS Rept. 1974, Sept. 1952. Alternatively see Hinze, J.O., Turbulence, McGraw-Hill, New York (1959) (Laufer's data in chapter 7).

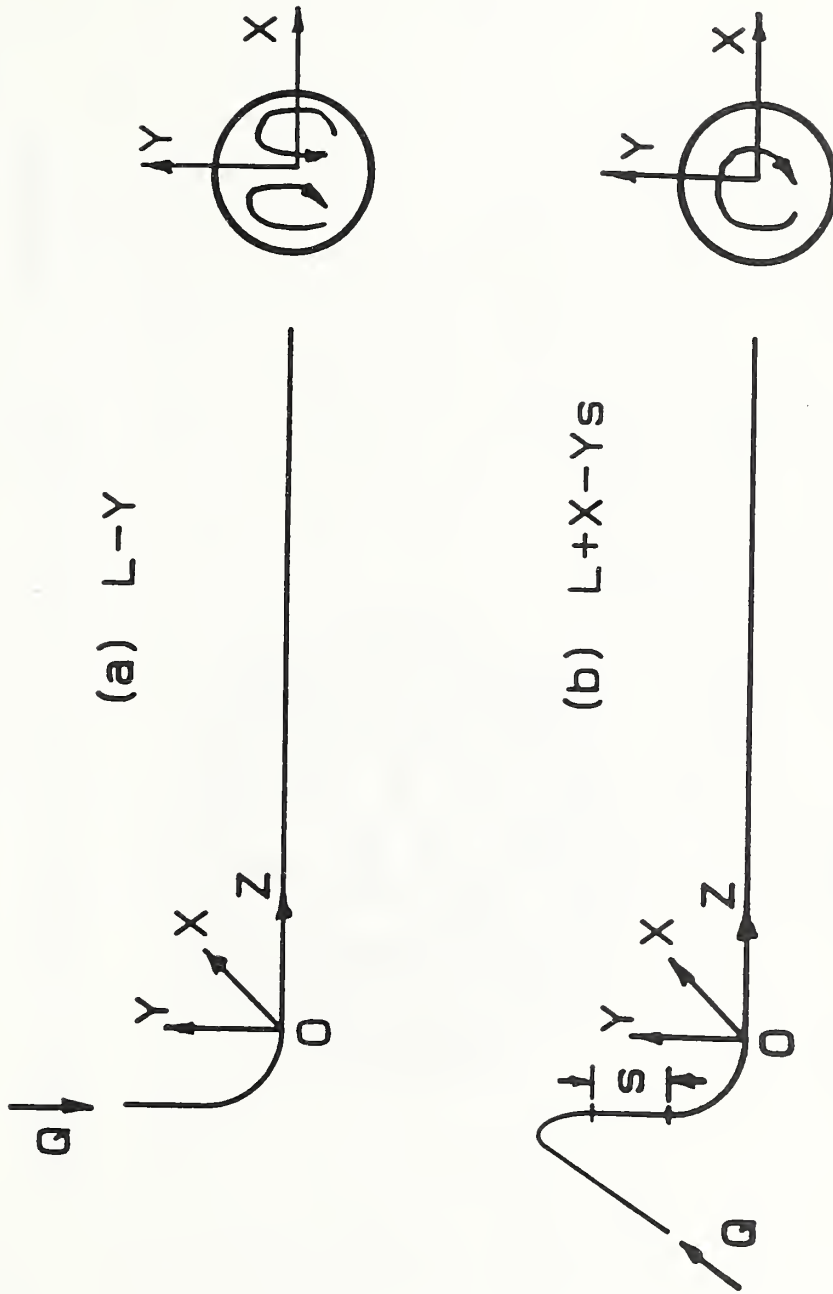


Figure 1. Sketch of Piping Configurations with Coordinate Systems and Sketched Distributions of the Swirl patterns Generated. (a) The Single Elbow, and (b) The Double Elbow Out-Of-Plane Configuration with Elbow Separation Denoted by Pipe Length "S" in Diameters.

19-Tube Bundle

$D = 52.5\text{mm}$

$L = 1.9D$

$d = 9.5\text{mm}$

$t = 0.4\text{mm}$

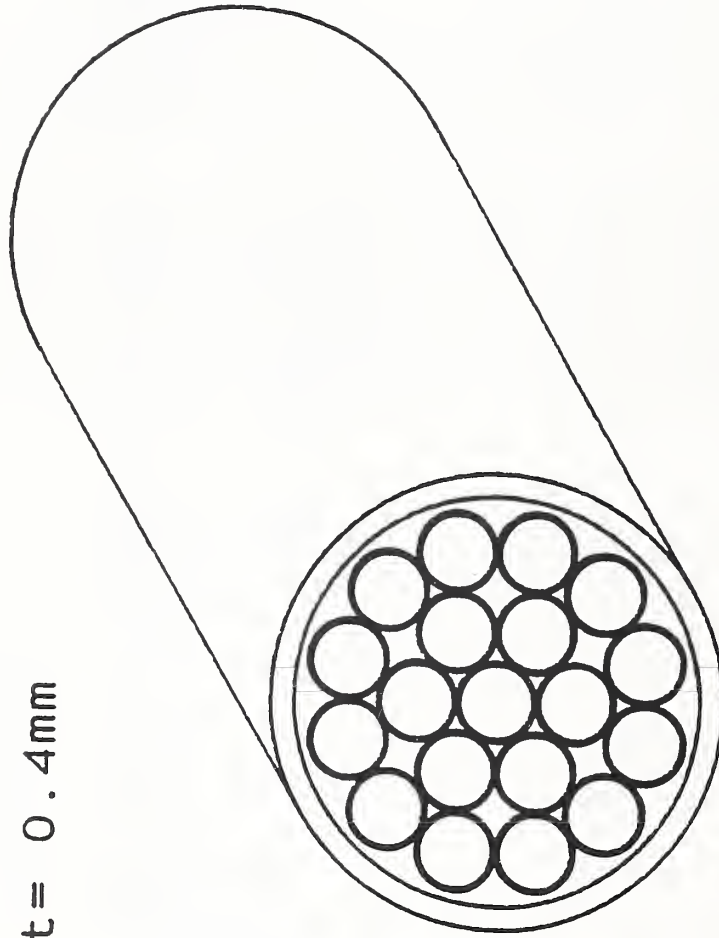


Figure 2. Sketch of the Tube Bundle Arrangement.

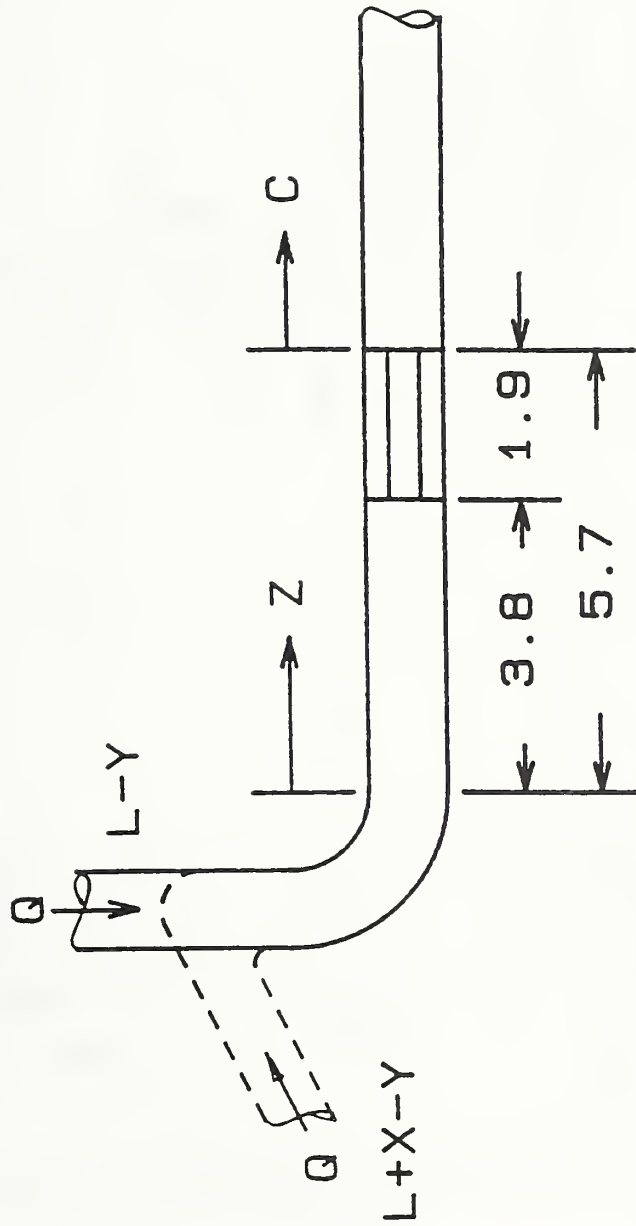


Figure 3. Sketch of Tube Bundle Installation Downstream of Single and Double Elbow Configurations. Dimensions are in Pipe Inside Diameters.

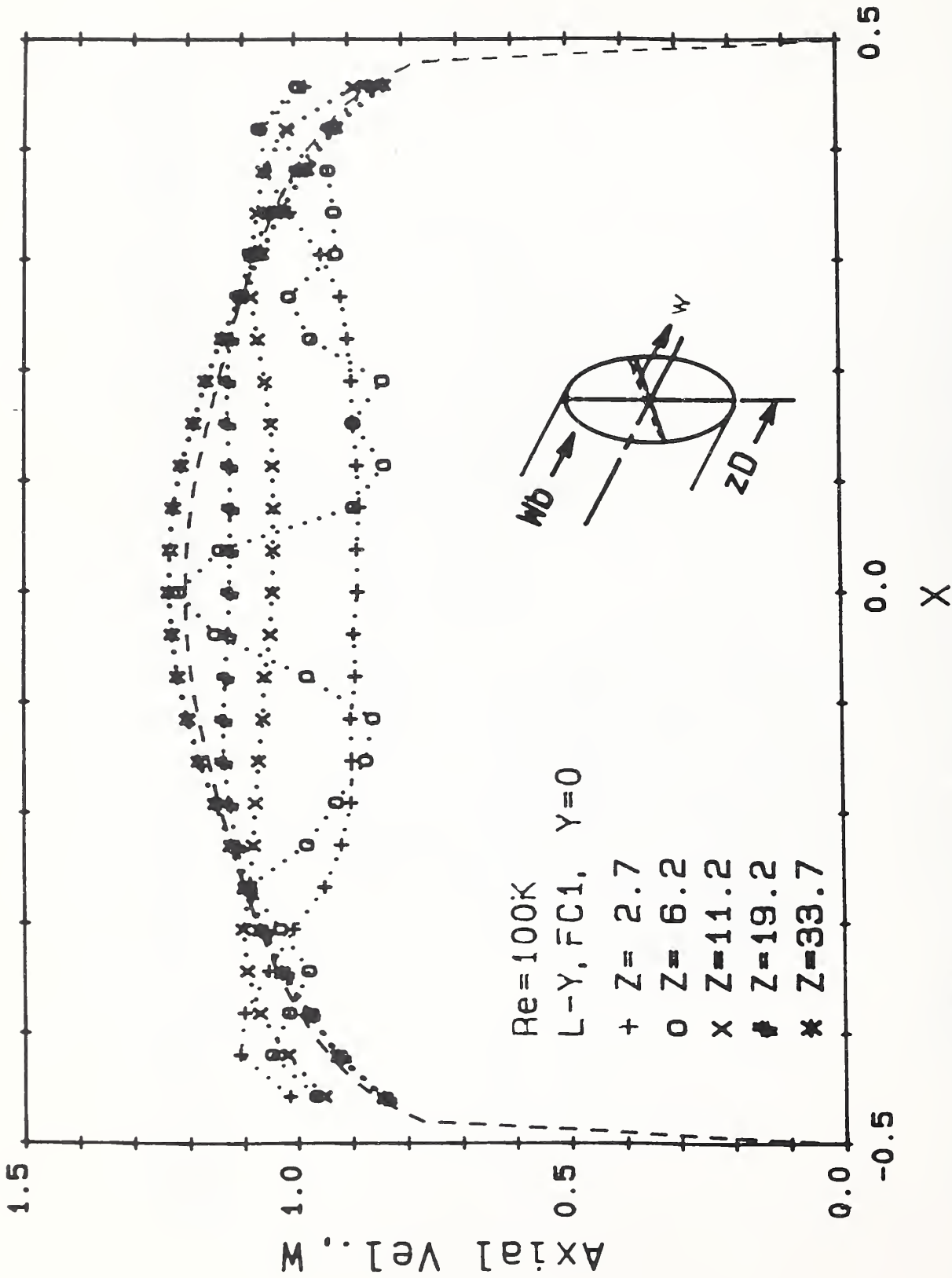


Figure 4. Axial Velocity Profile Results vs. Horizontal Radial Position at Different Downstream Locations for the Single Elbow and Tube Bundle Arrangement for $Re = 100K$.

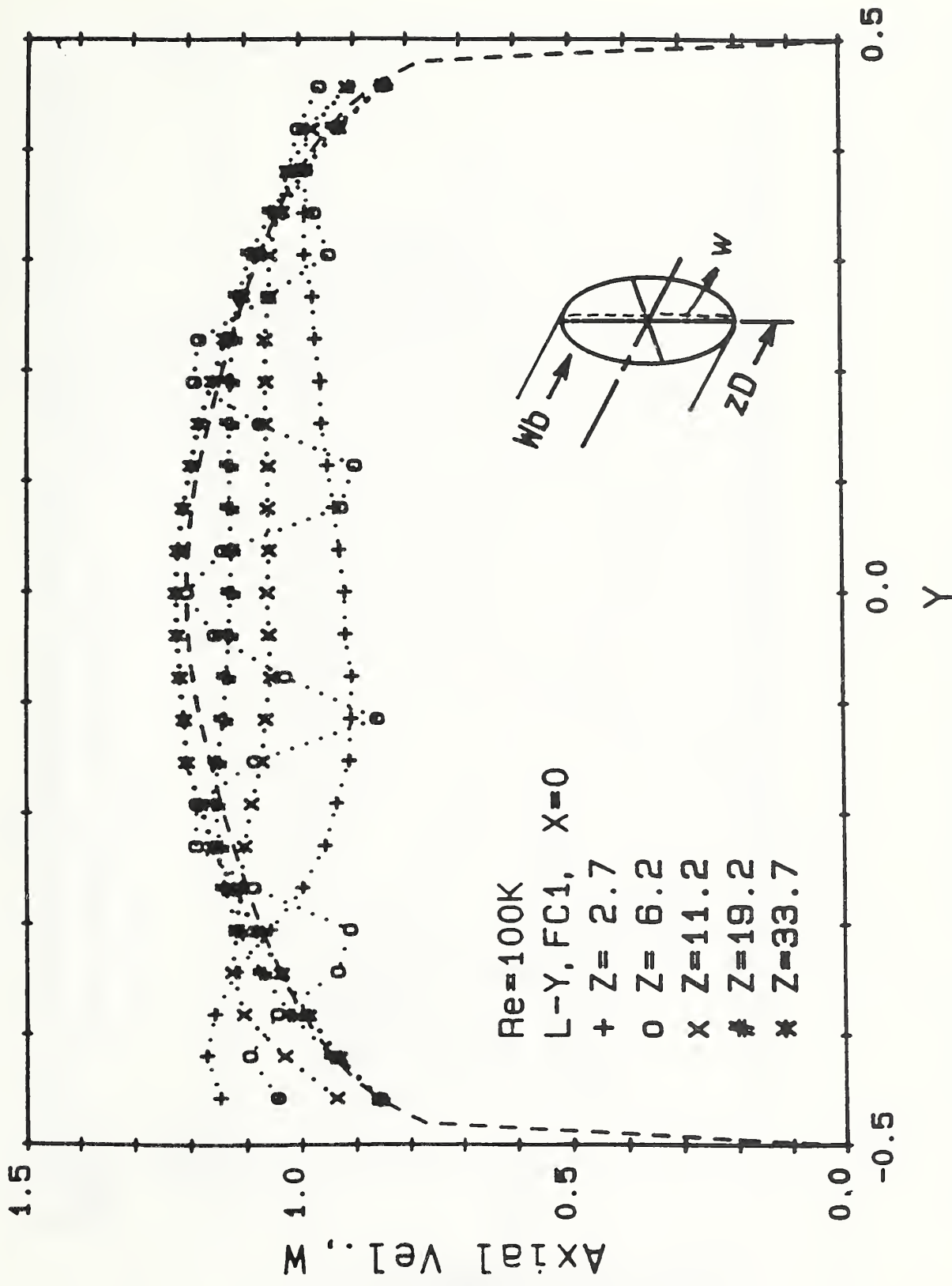


Figure 5. Axial Velocity Profile Results vs. Vertical Radial Position at Different Downstream Locations for the Single Elbow and Tube Bundle Arrangement for $Re = 100K$.

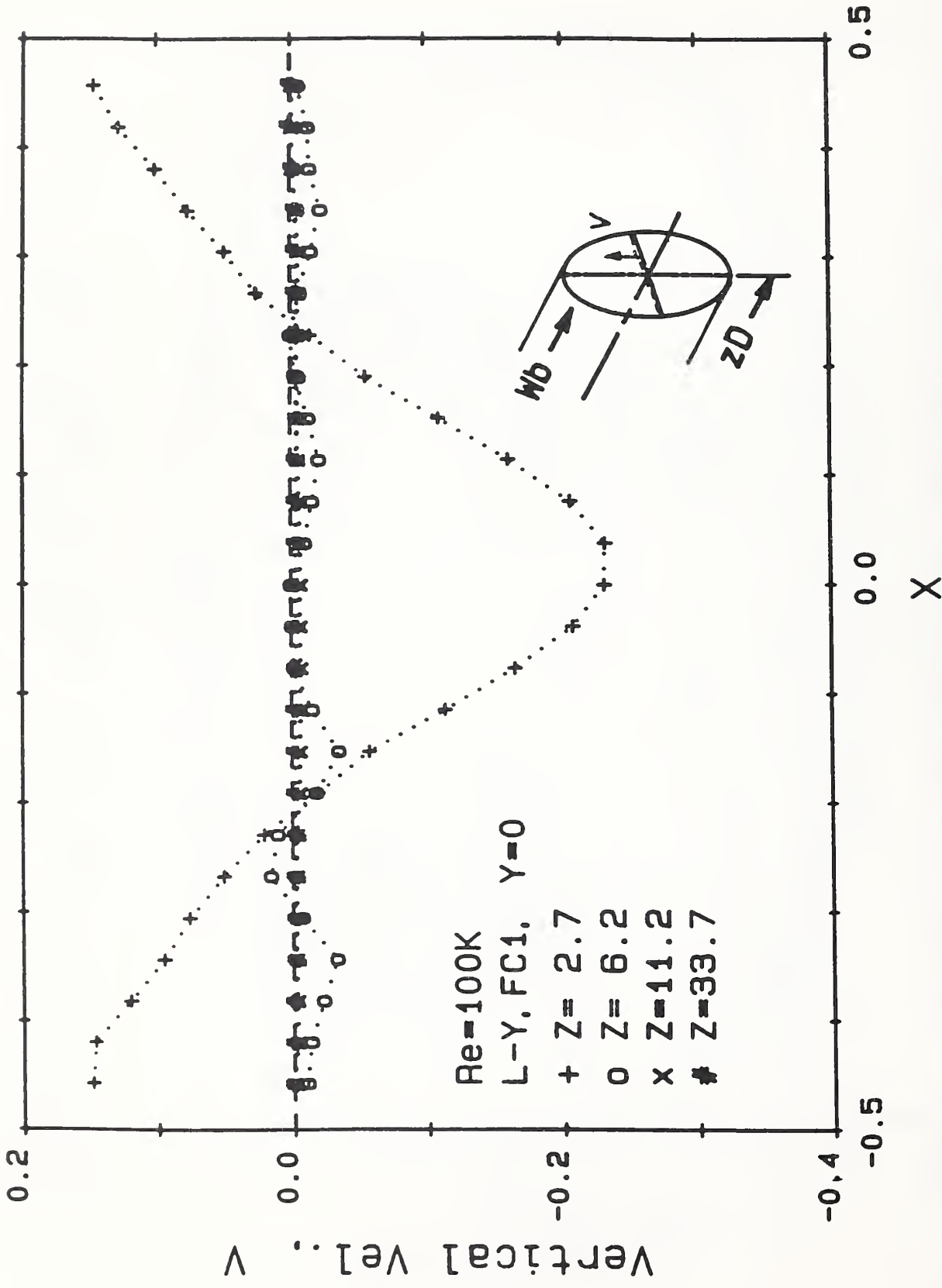


Figure 6. Vertical Velocity Profile Results vs. Horizontal Radial Position at Different Downstream Locations for the Single Elbow and Tube Bundle Arrangement for Re = 100K.

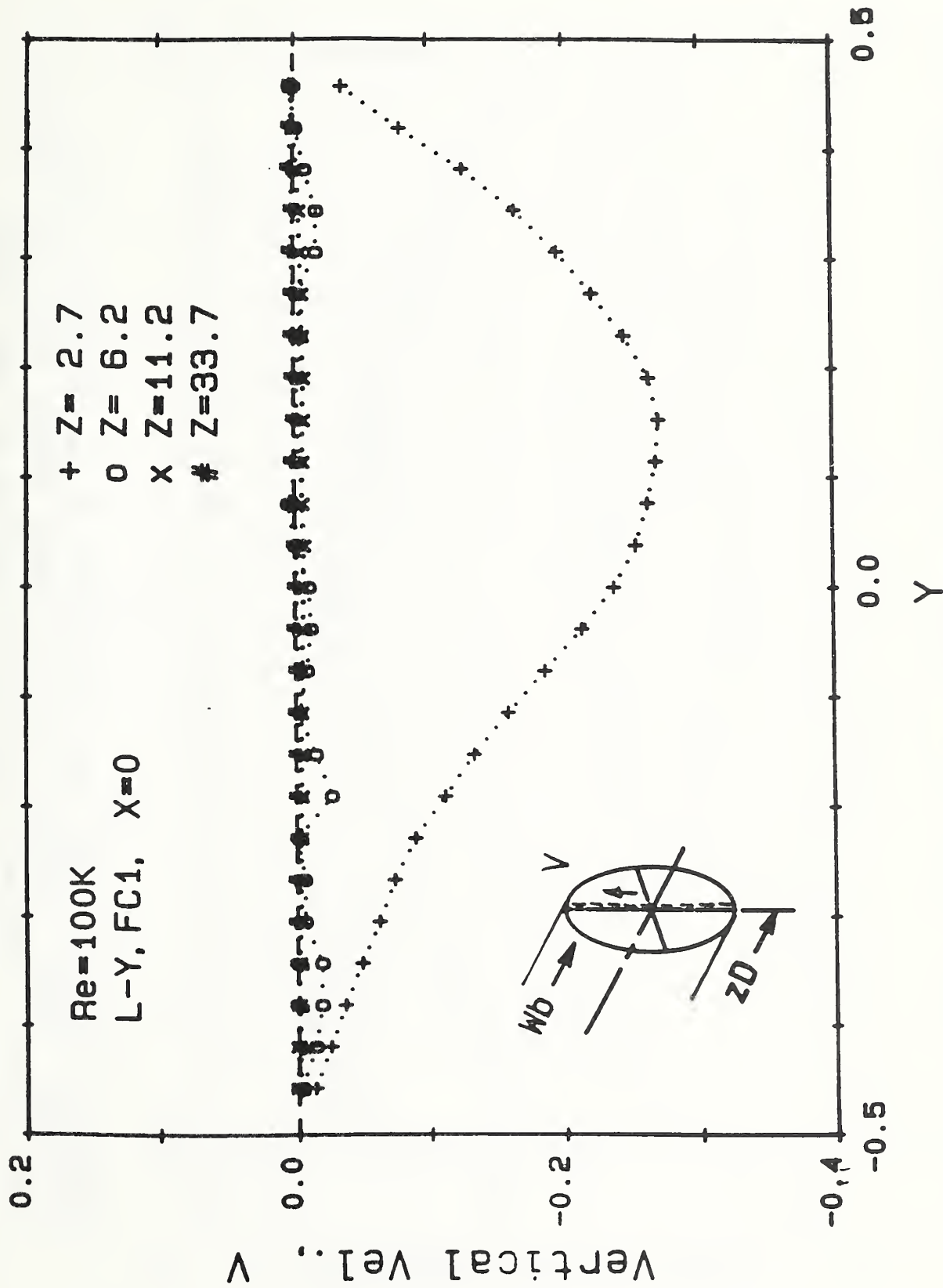


Figure 7. Vertical Velocity Profile Results vs. Vertical Radial Position at Different Downstream Locations for the Single Elbow and Tube Bundle Arrangement for $Re = 100K$.

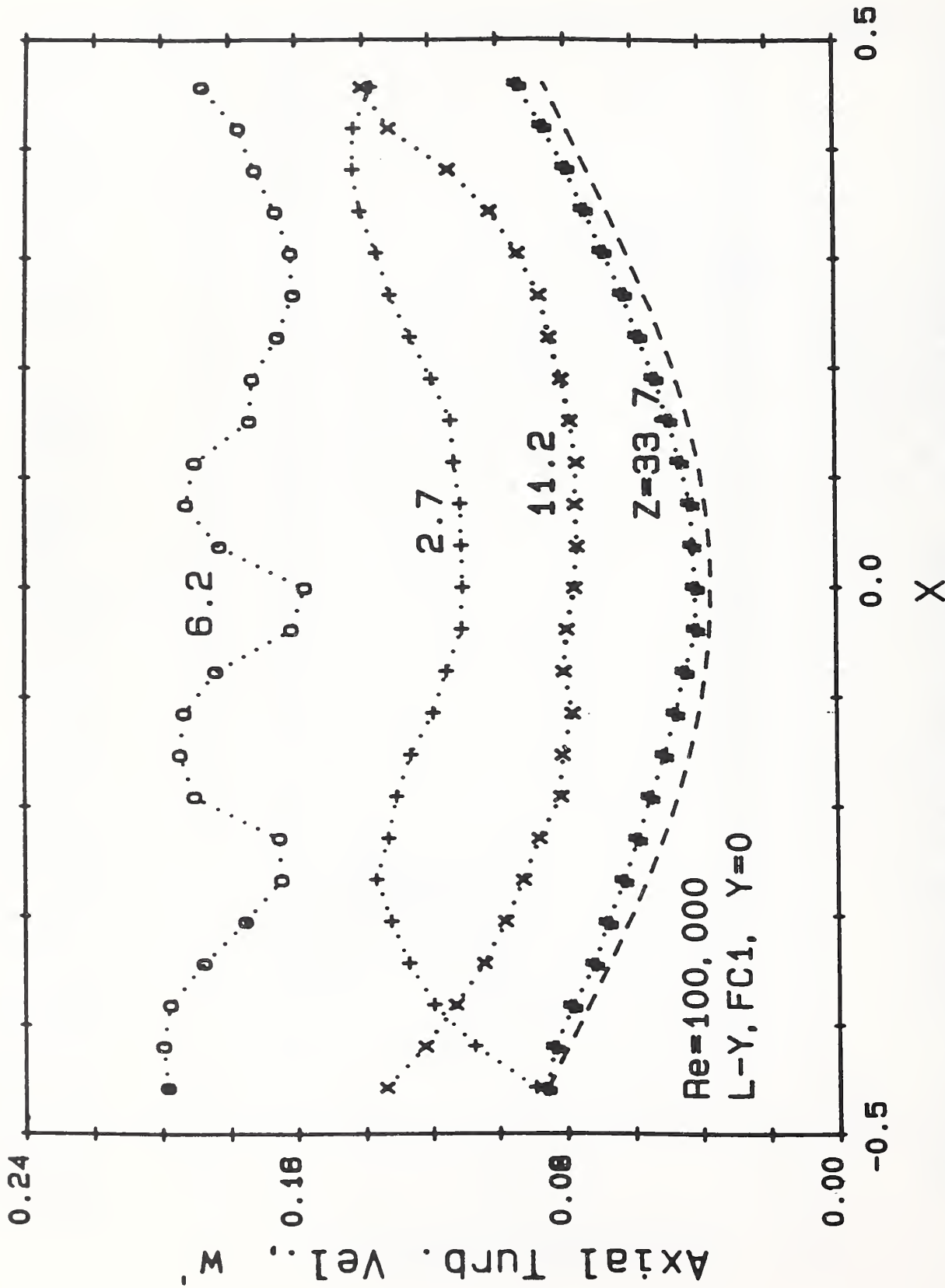


Figure 8. Profiles of the Axial Component of the Turbulent Velocity vs. Horizontal Radial Position for the Single Elbow and Tube Bundle Arrangement at Different Downstream Locations for $Re = 100K$.

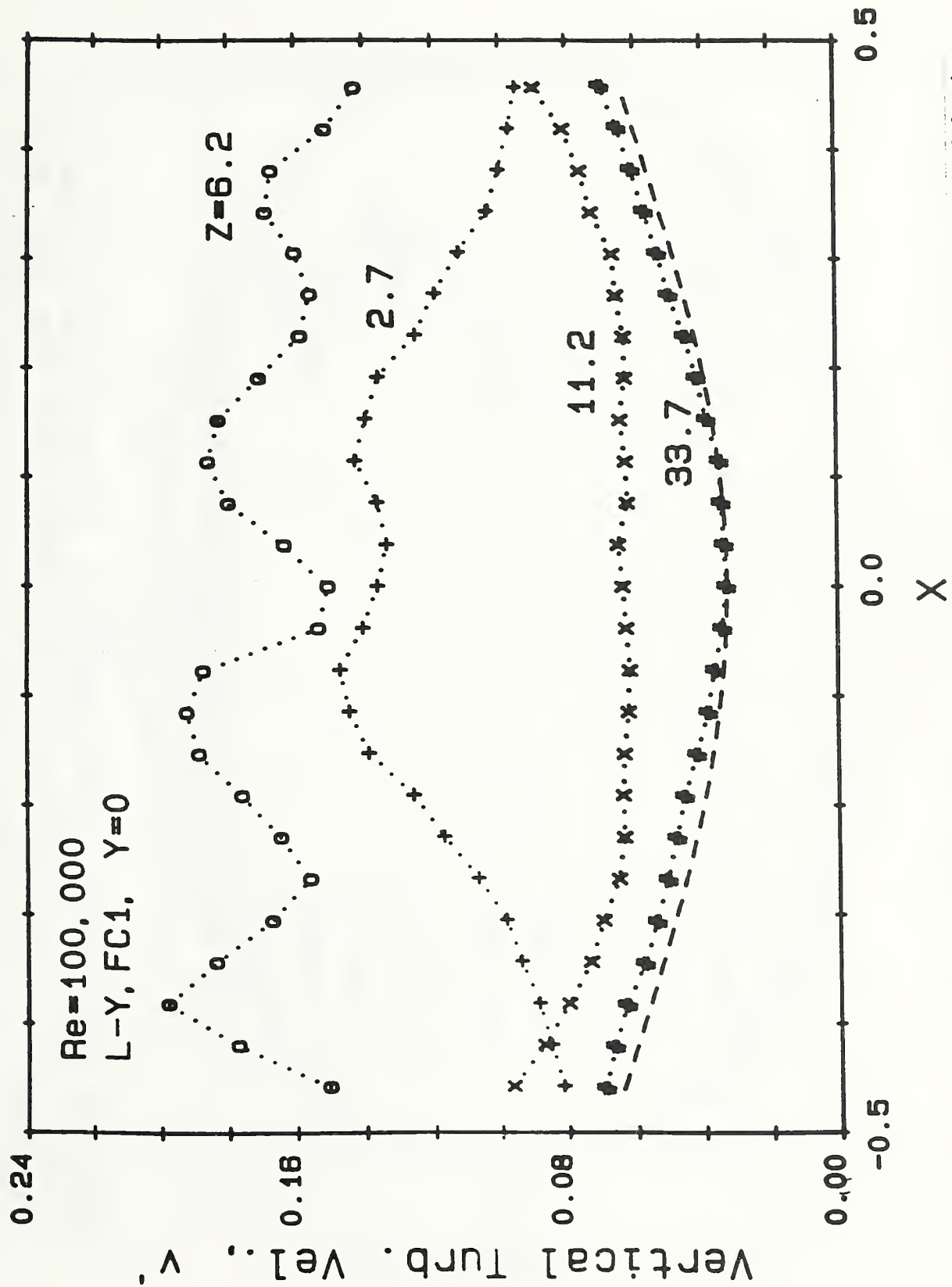


Figure 9. Profiles of the Vertical Component of the Turbulent Velocity vs. Horizontal Radial Position at Different Downstream Locations for the Single Elbow and Tube Bundle Arrangements for $Re = 100K$.

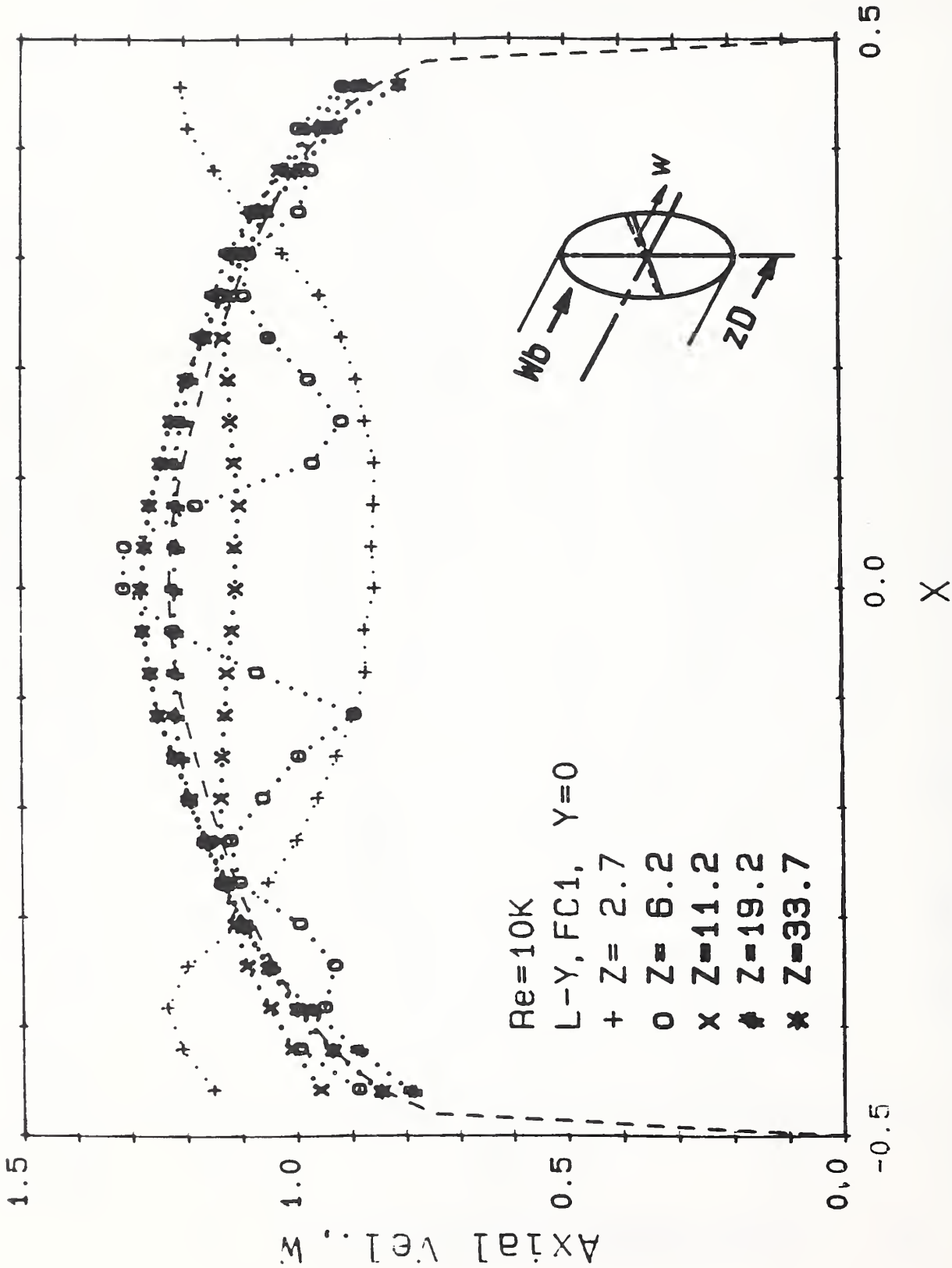


Figure 10. Axial Velocity Profile Results vs. Horizontal Radial Position at Different Downstream Locations for the Single Elbow and Tube Bundle Arrangement for $Re = 10K$.

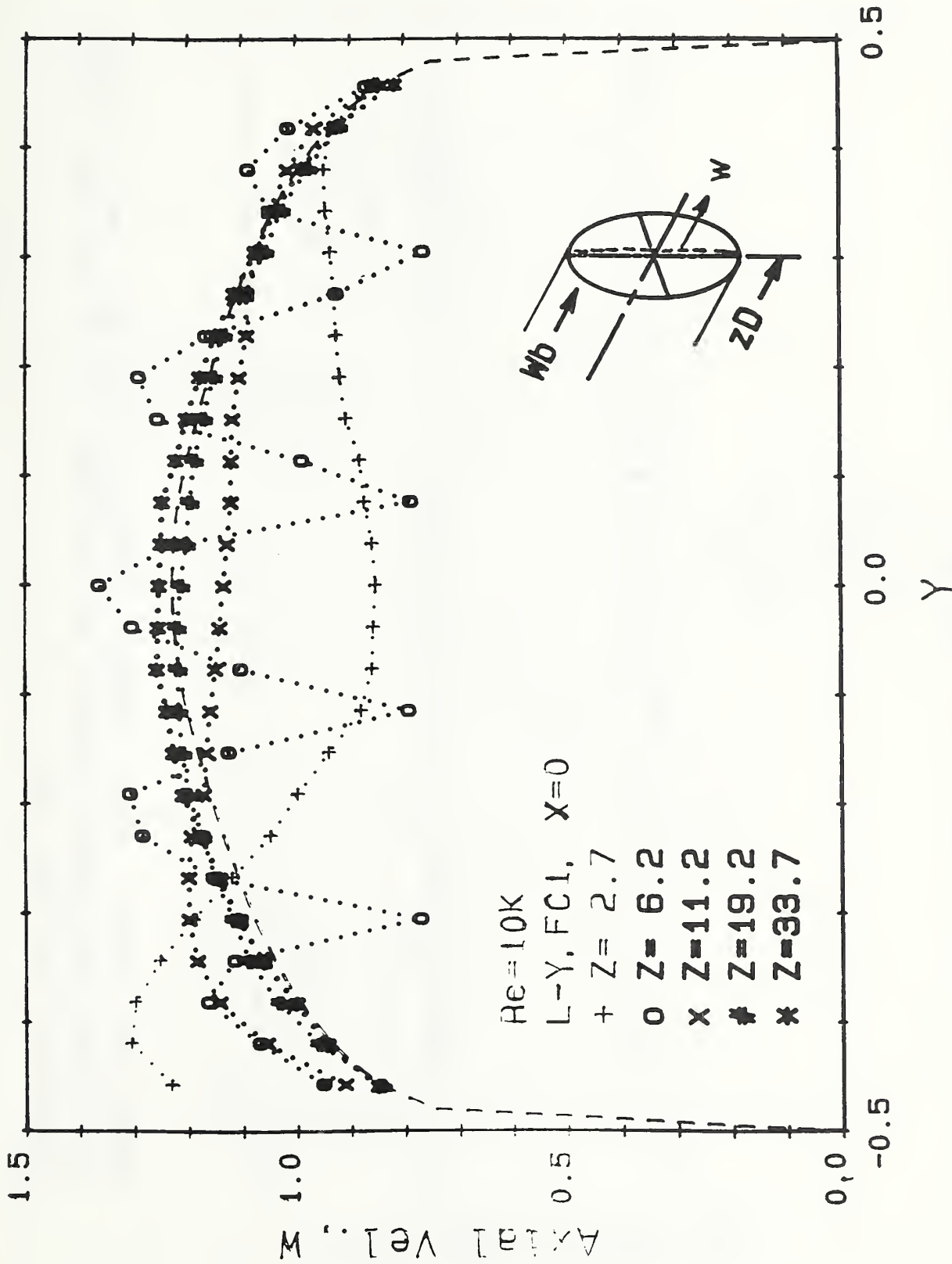


Figure 11. Axial Velocity Profile Results vs. Vertical Radial Position at Different Downstream Locations for the Single Elbow and Tube Bundle Arrangement for $Re = 10K$.

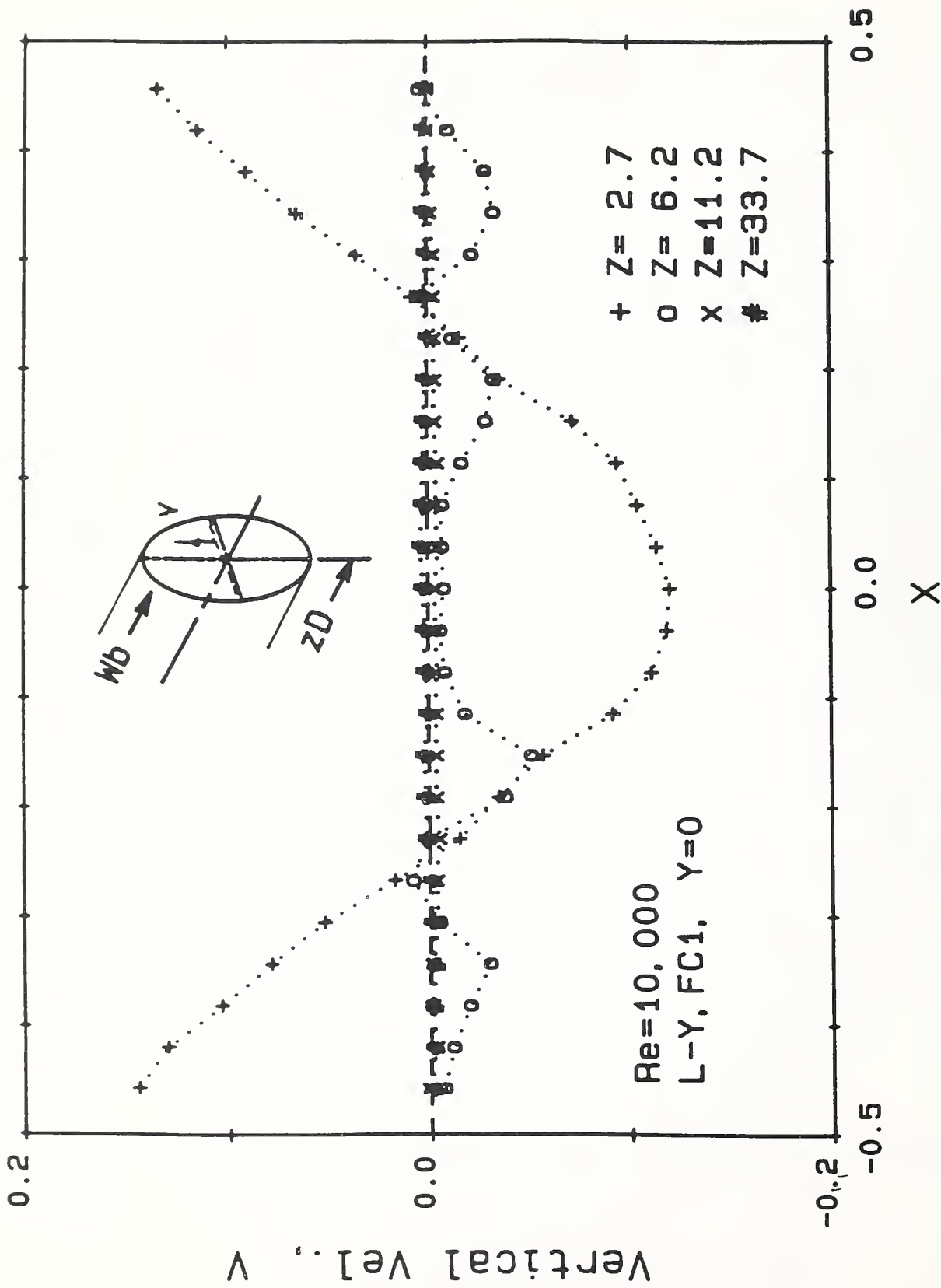


Figure 12. Vertical Velocity Profile Results vs. Horizontal Radial Position at Different Downstream Locations for the Single Elbow and Tube Bundle Arrangement for $Re = 10K$.

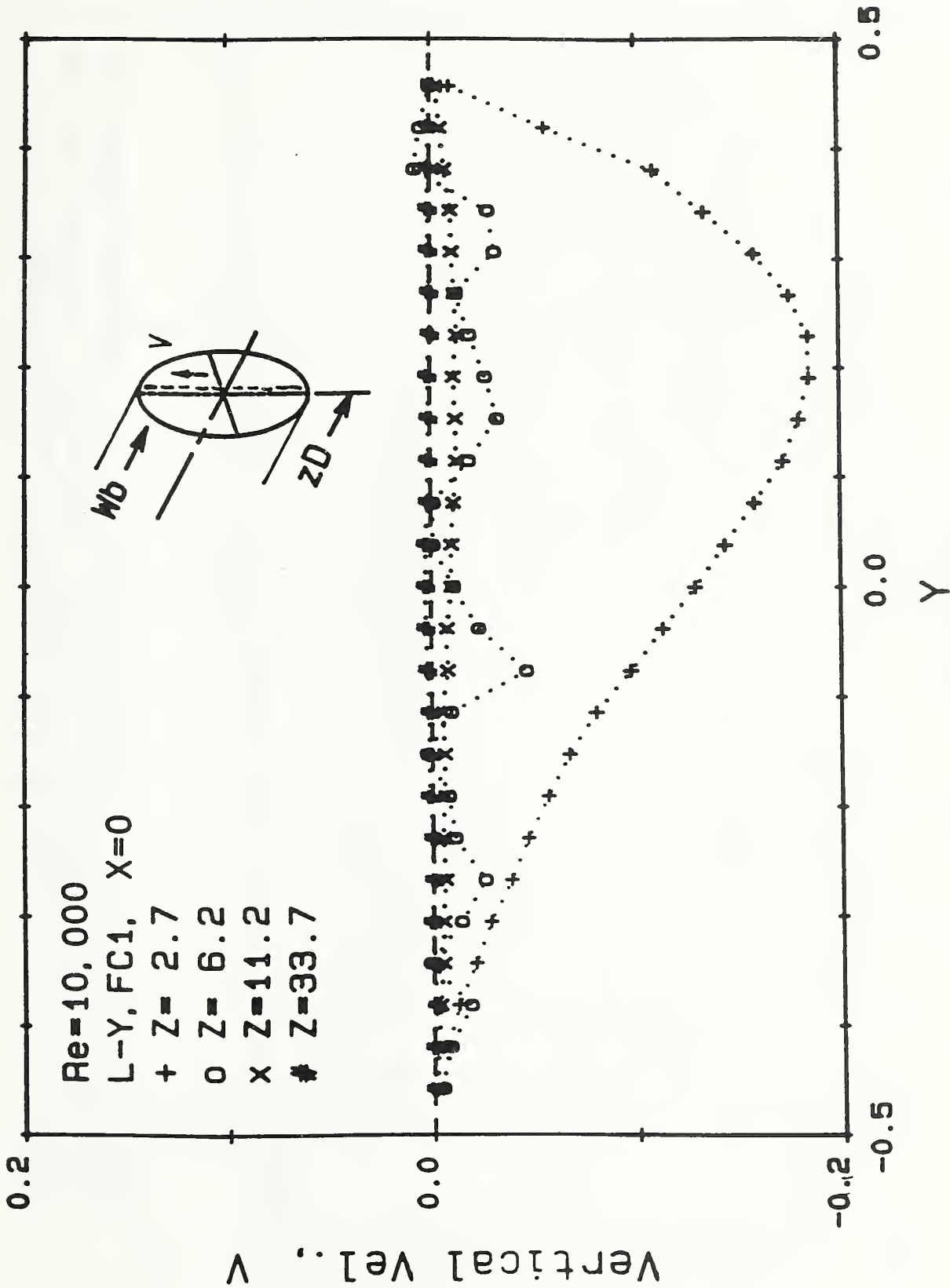


Figure 13. Vertical Velocity Profile Results vs. Vertical Radial Position at Different Downstream Locations for the Single Elbow and Tube Bundle Arrangement for $Re = 10K$.

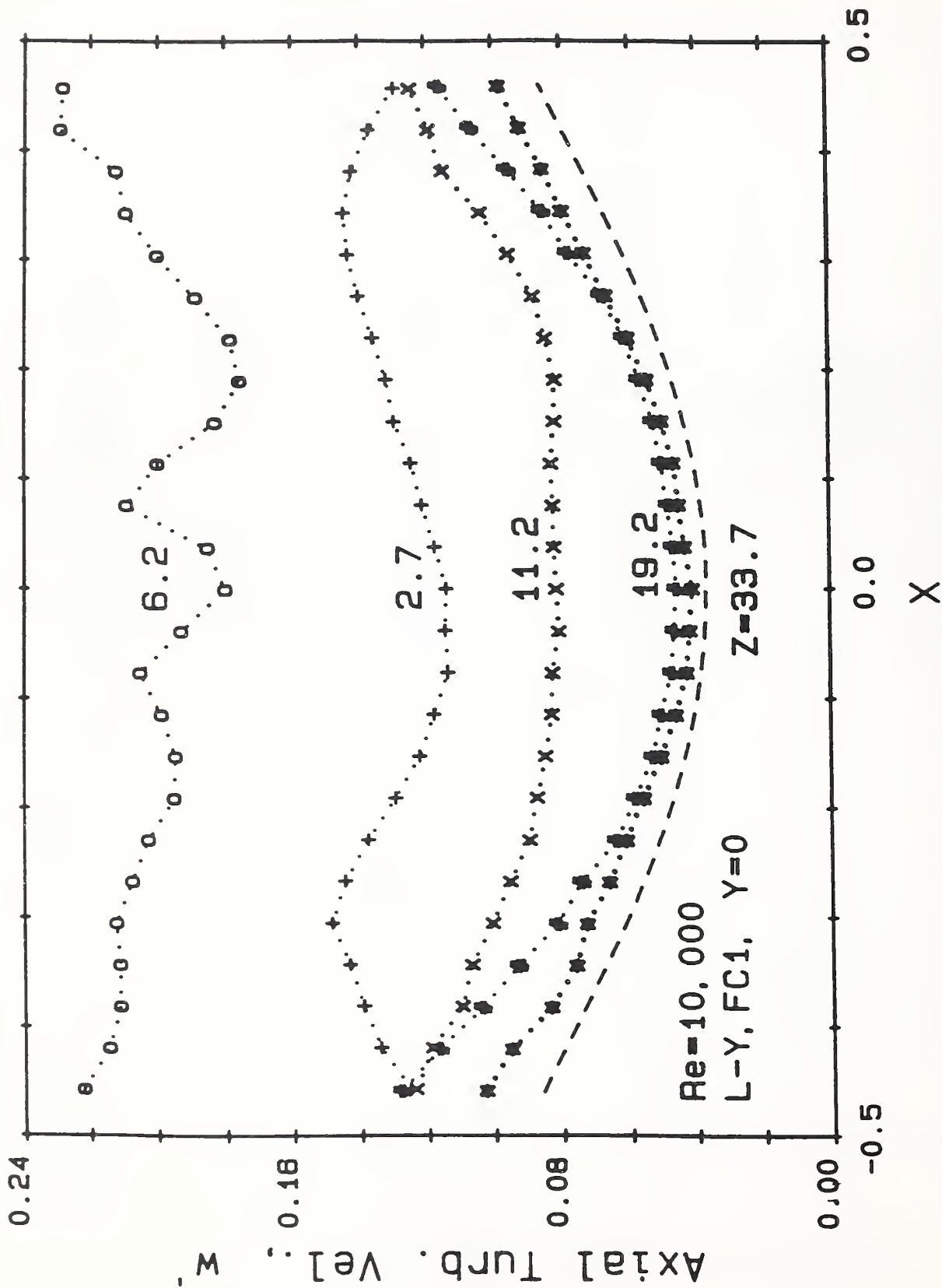


Figure 14. Profiles of the Axial Component of the Turbulent Velocity vs. Horizontal Radial Position at Different Downstream Locations for the Single Elbow and Tube Bundle Arrangement for $Re = 10K$.

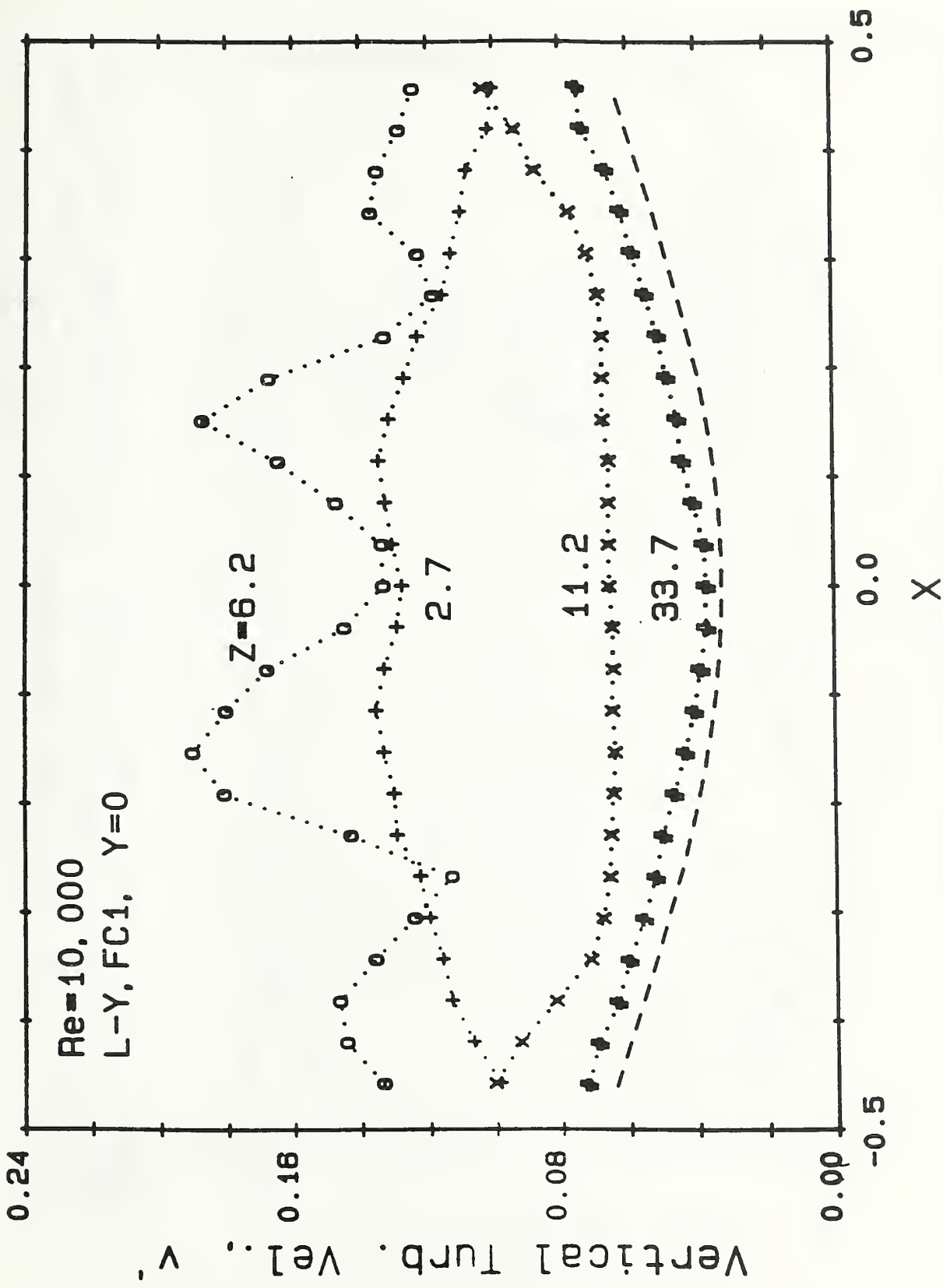


Figure 15. Profiles of the Vertical Component of the Turbulent Velocity vs. Horizontal Radial Position at Different Downstream Locations for the Single Elbow and Tube Bundle Arrangement for $Re = 10K$.

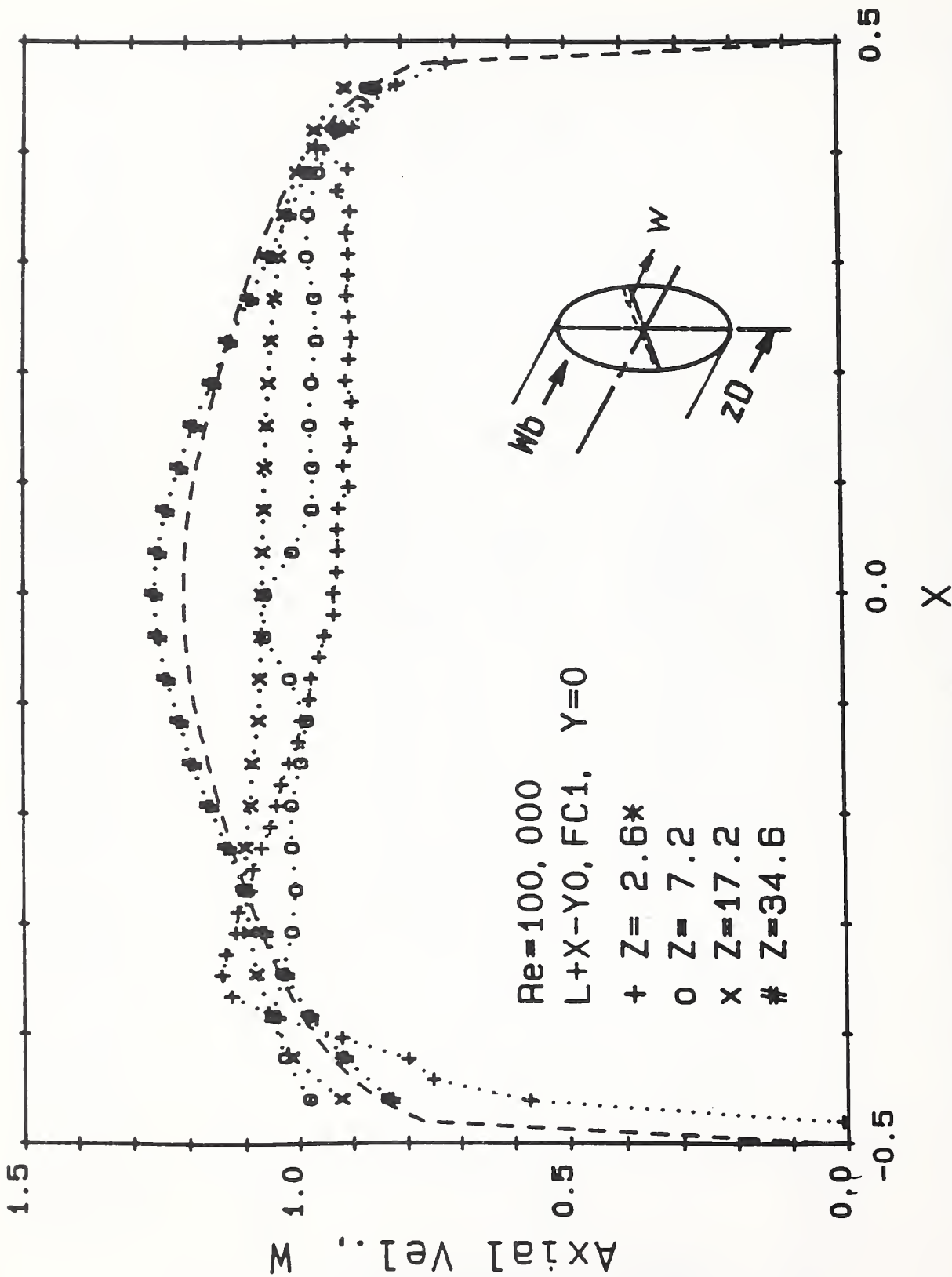


Figure 16. Axial Velocity Profile Results vs. Horizontal Radial Position at Different Downstream Locations for the Closely Coupled Double Elbow-Out-Of-Plane and Tube Bundle Arrangement for Re = 100K.

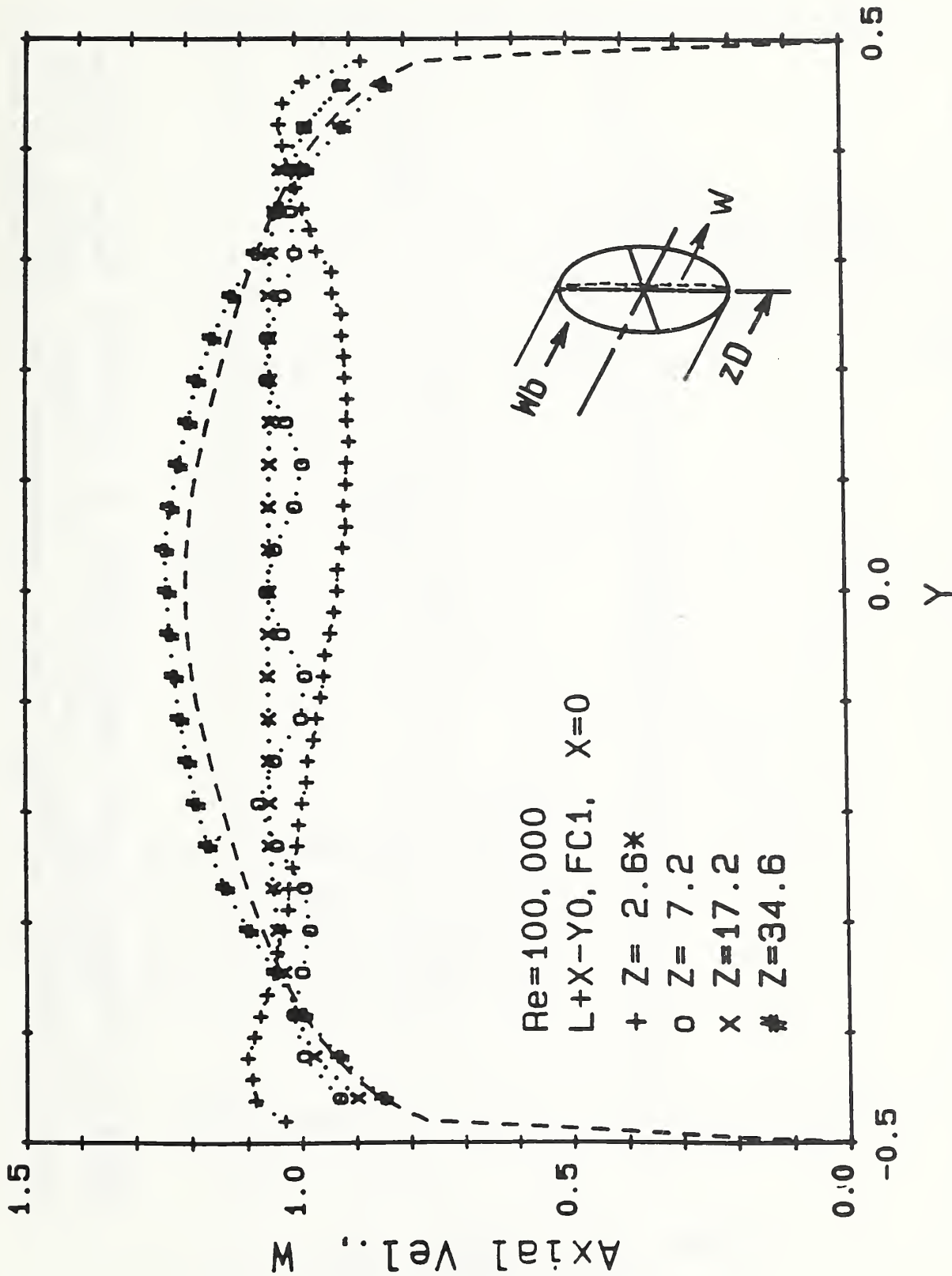


Figure 17. Axial Velocity Profile Results vs. Vertical Radial Position at Different Downstream Locations for the Closely Coupled Double Elbows-Out-Of-Plane and Tube Bundle Arrangement for $Re = 100K$.

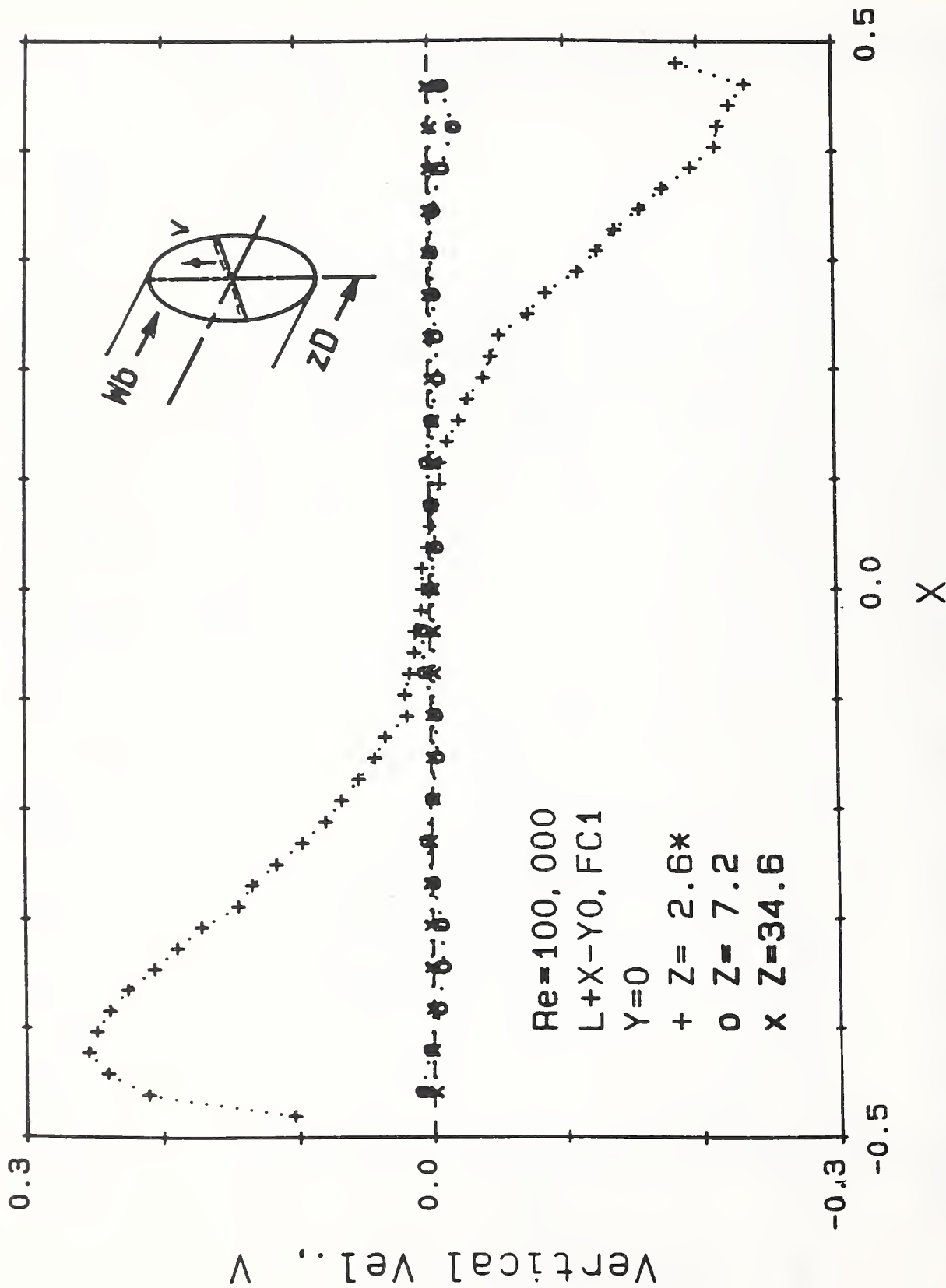


Figure 18. Vertical Velocity Profile Results vs. Horizontal Radial Position at Different Downstream Locations for the Closely Coupled Double Elbows-Out-Of-Plane and Tube Bundle Arrangement for $Re = 100K$.

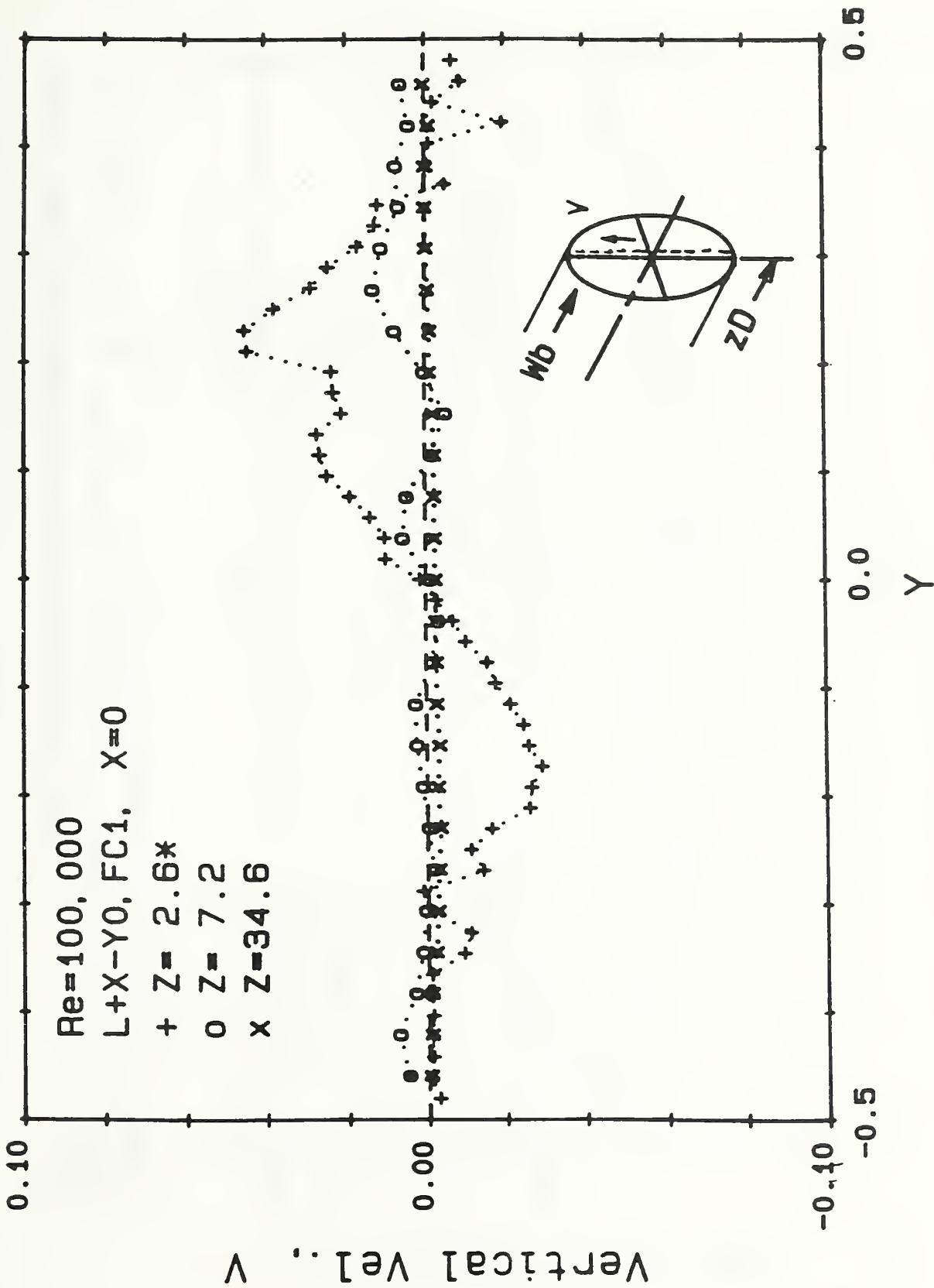


Figure 19. Vertical Velocity Profile Results vs. Vertical Radial Position at Different Downstream Locations for the Closely Coupled Double Elbows-Out-Of-Plane and Tube Bundle Arrangement for $Re = 100K$.

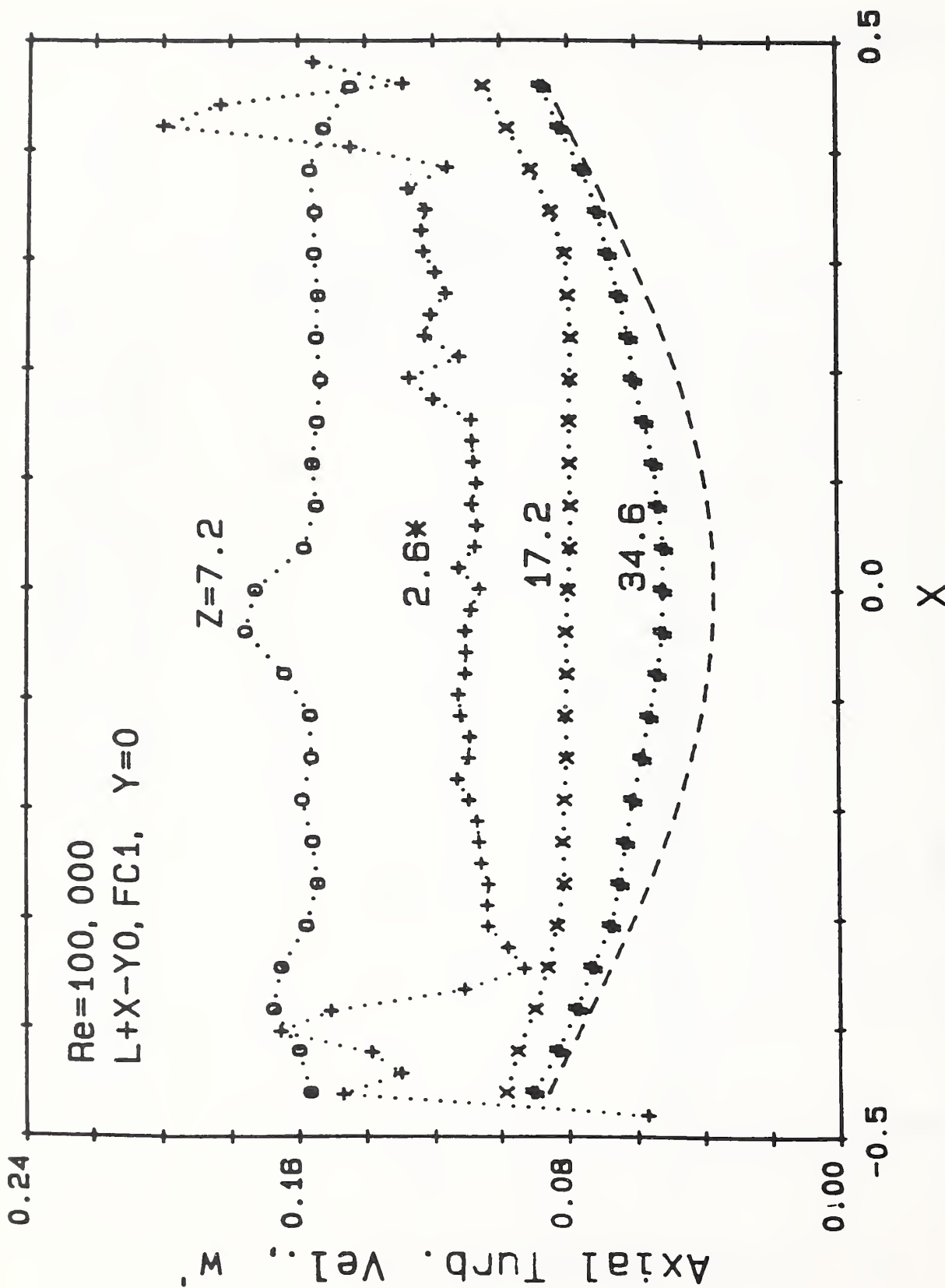


Figure 20. Profiles of the Axial Component of the Turbulent Velocity vs. Horizontal Radial Position at Different Downstream Locations for the Double Elbows-Out-Of-Plane and Tube Bundle Arrangement for $Re = 100K$.

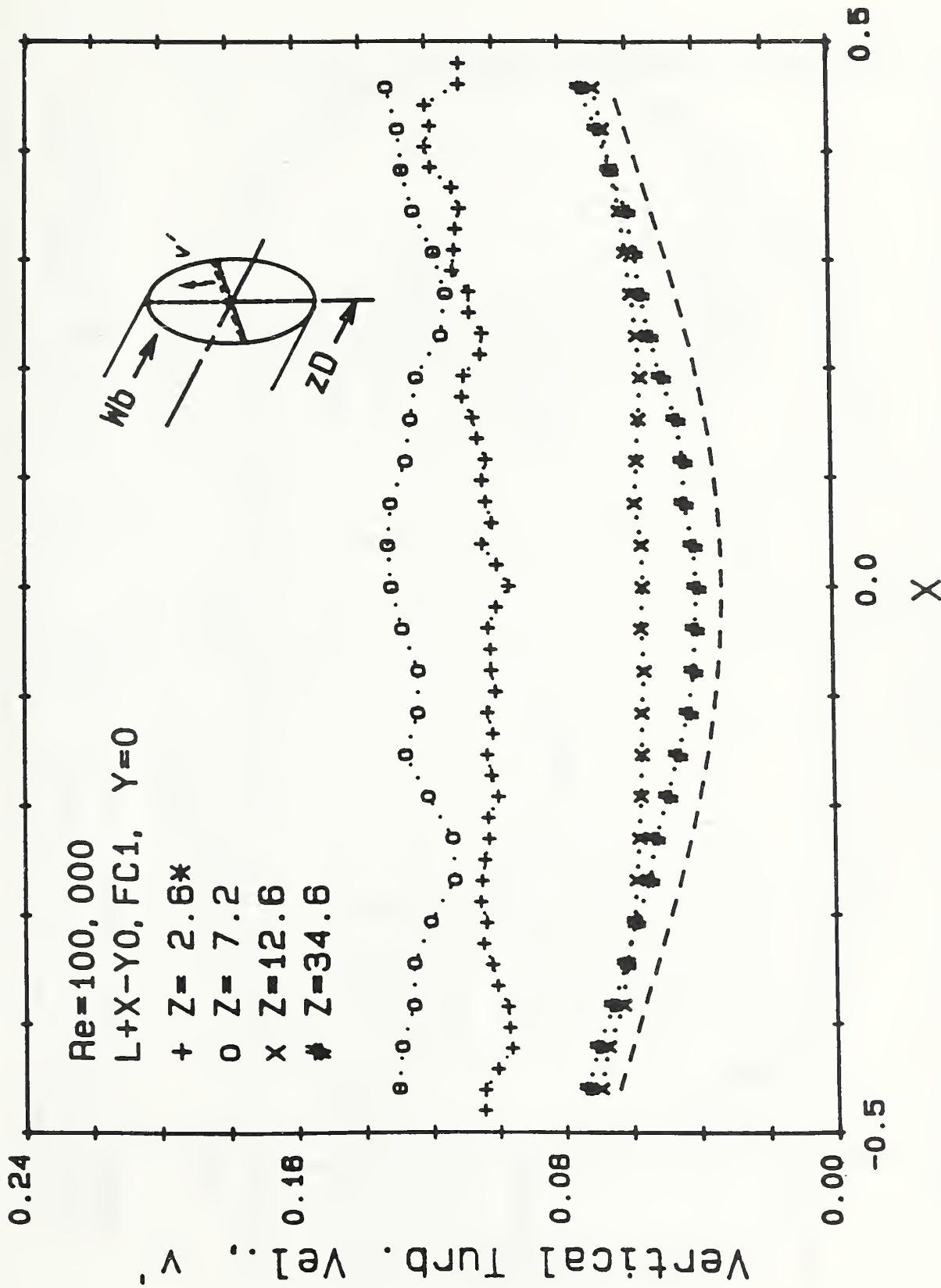


Figure 21. Profiles of the Vertical Component of the Turbulent Velocity vs. Horizontal Radial Position at Different Downstream Locations for the Double Elbows-Out-Of-Plane and Tube Bundle Arrangement for Re = 100K.

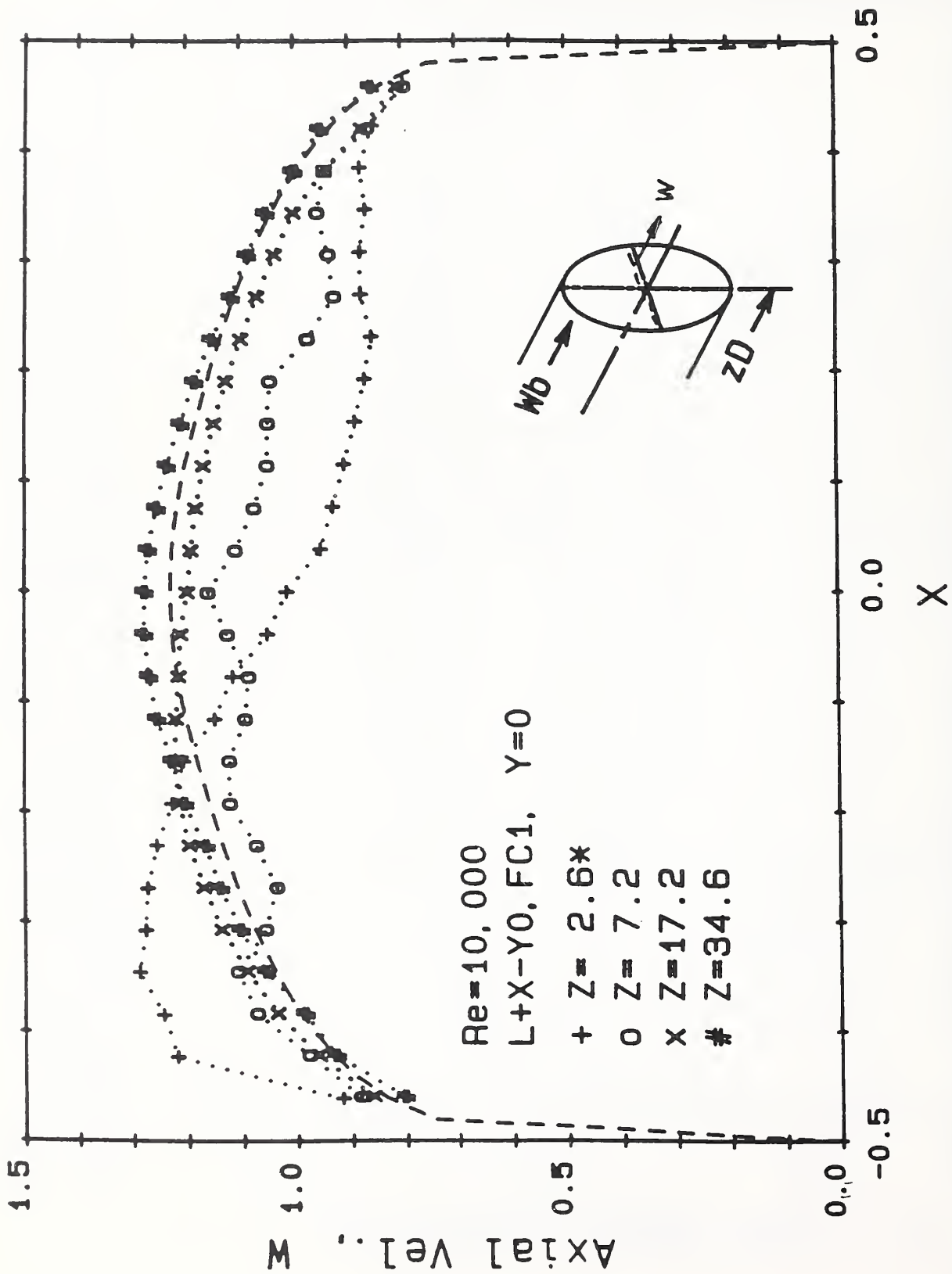


Figure 22. Axial Velocity Profile Results vs. Horizontal Radial Position at Different Downstream Locations for the Closely Coupled Double Elbow-Out-Of-Plane and Tube Bundle Arrangement for $Re = 10K$.

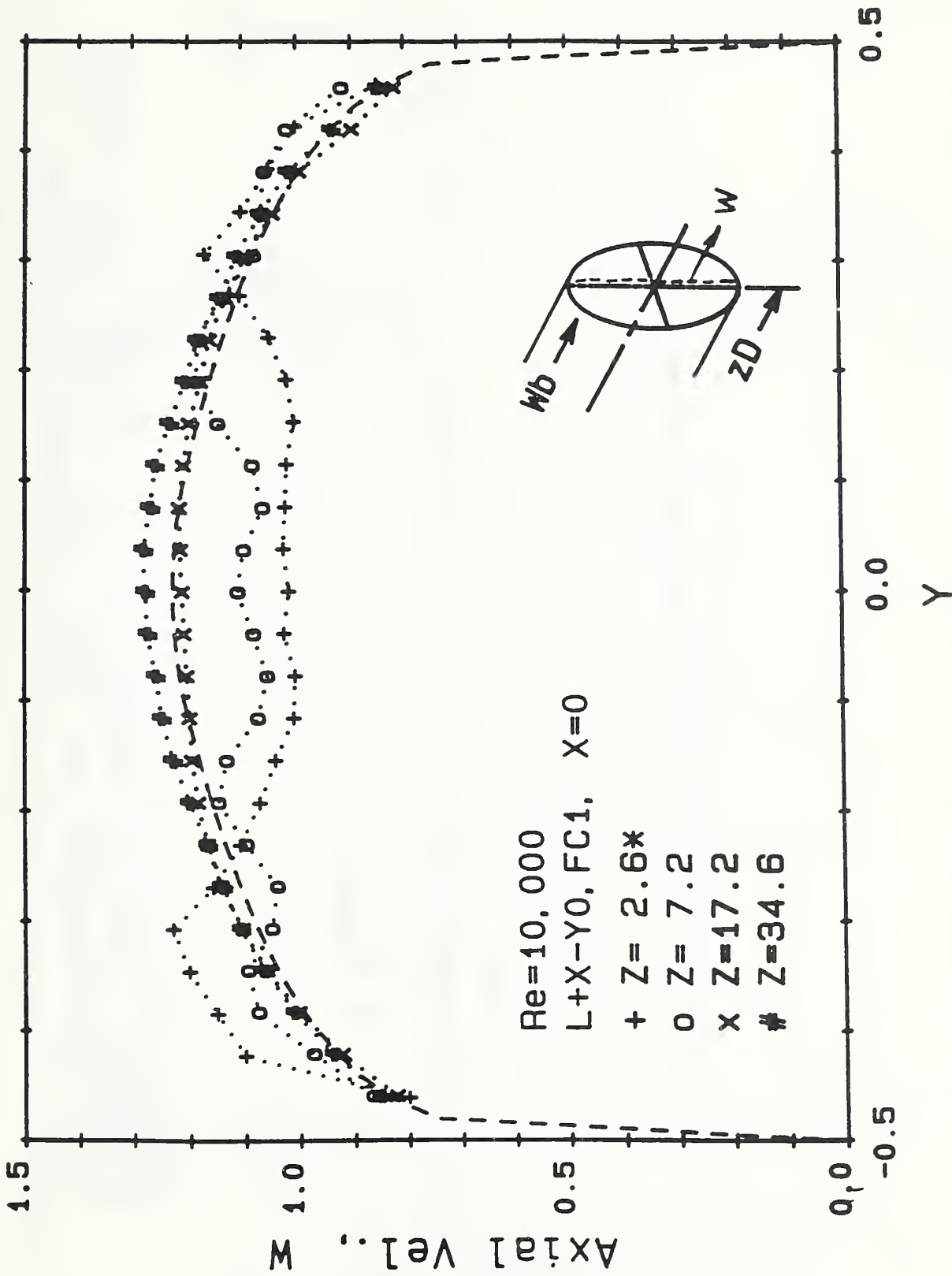


Figure 23. Axial Velocity Profile Results vs. Vertical Radial Position at Different Downstream Locations for the Closely Coupled Double Elbows-Out-Of-Plane and Tube Bundle Arrangement for $Re = 10K$.

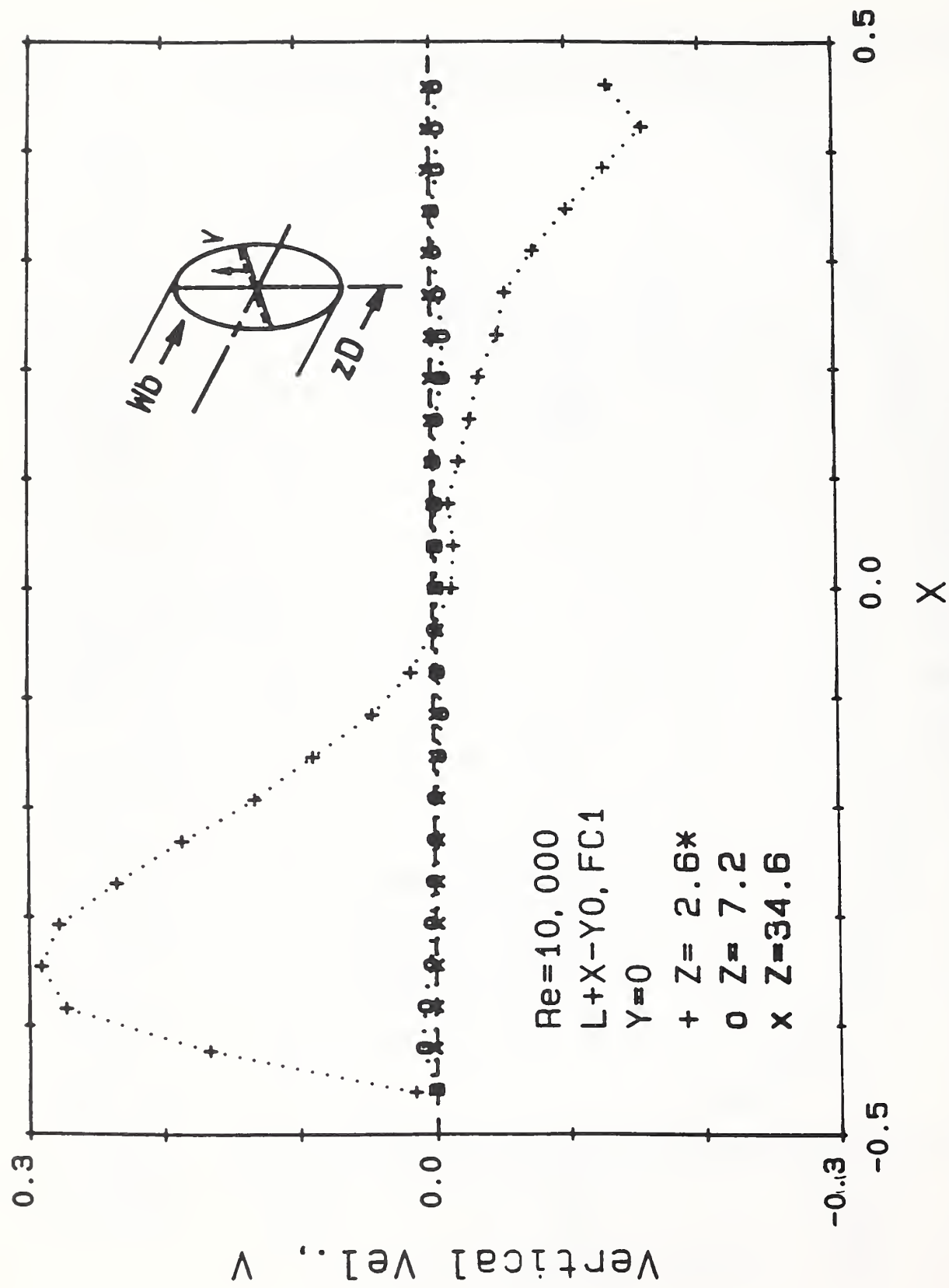


Figure 24. Vertical Velocity Profile Results vs. Horizontal Radial Position at Different Downstream Locations for the Closely Coupled Double Elbows-Out-Of-Plane and Tube Bundle Arrangement for $Re = 10K$.

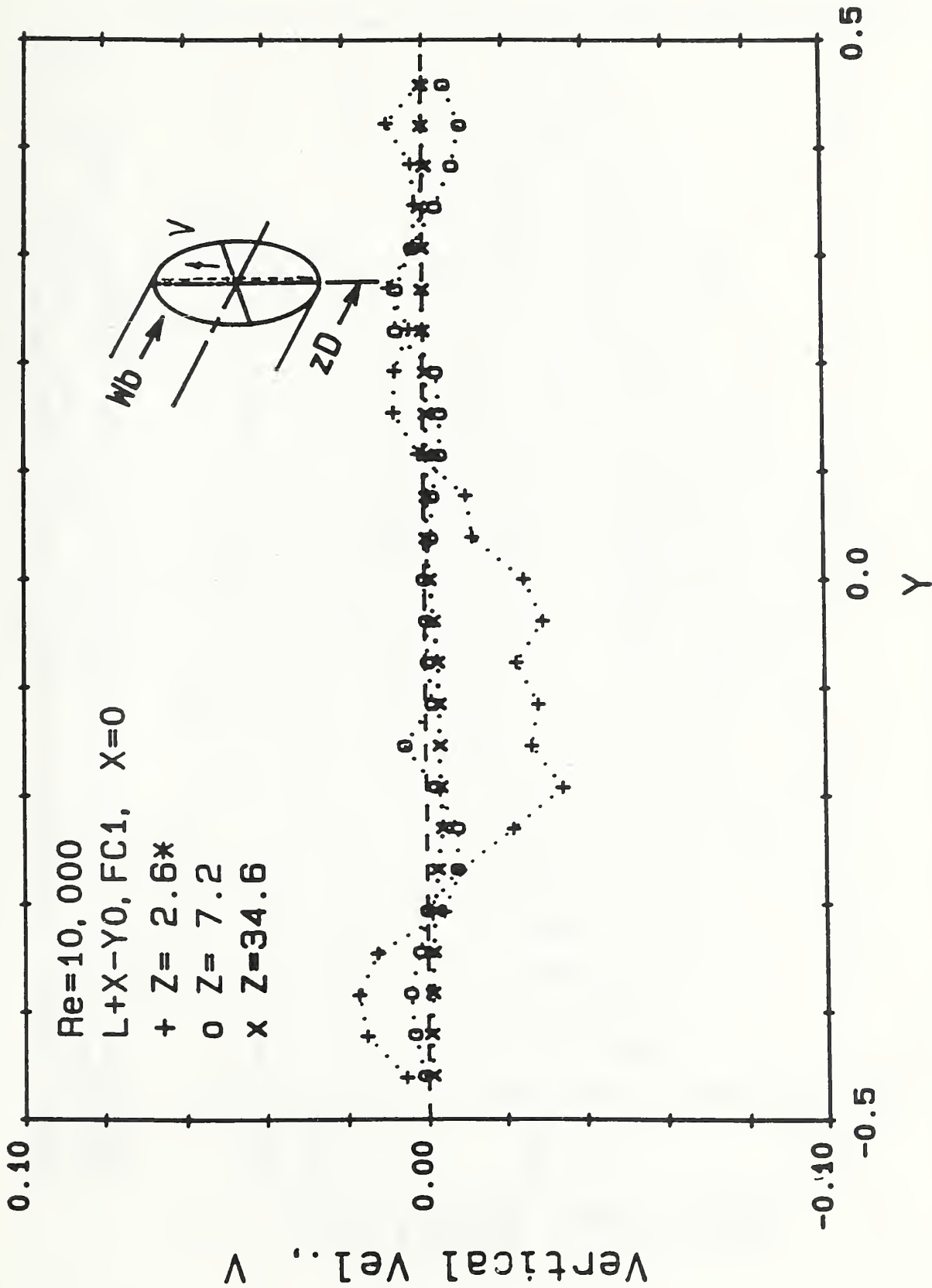


Figure 25. Vertical Velocity Profile Results vs. Vertical Radial Position at Different Downstream Locations for the Closely Coupled Double Elbows-Out-Of-Plane and Tube Bundle Arrangement for Re = 10K.

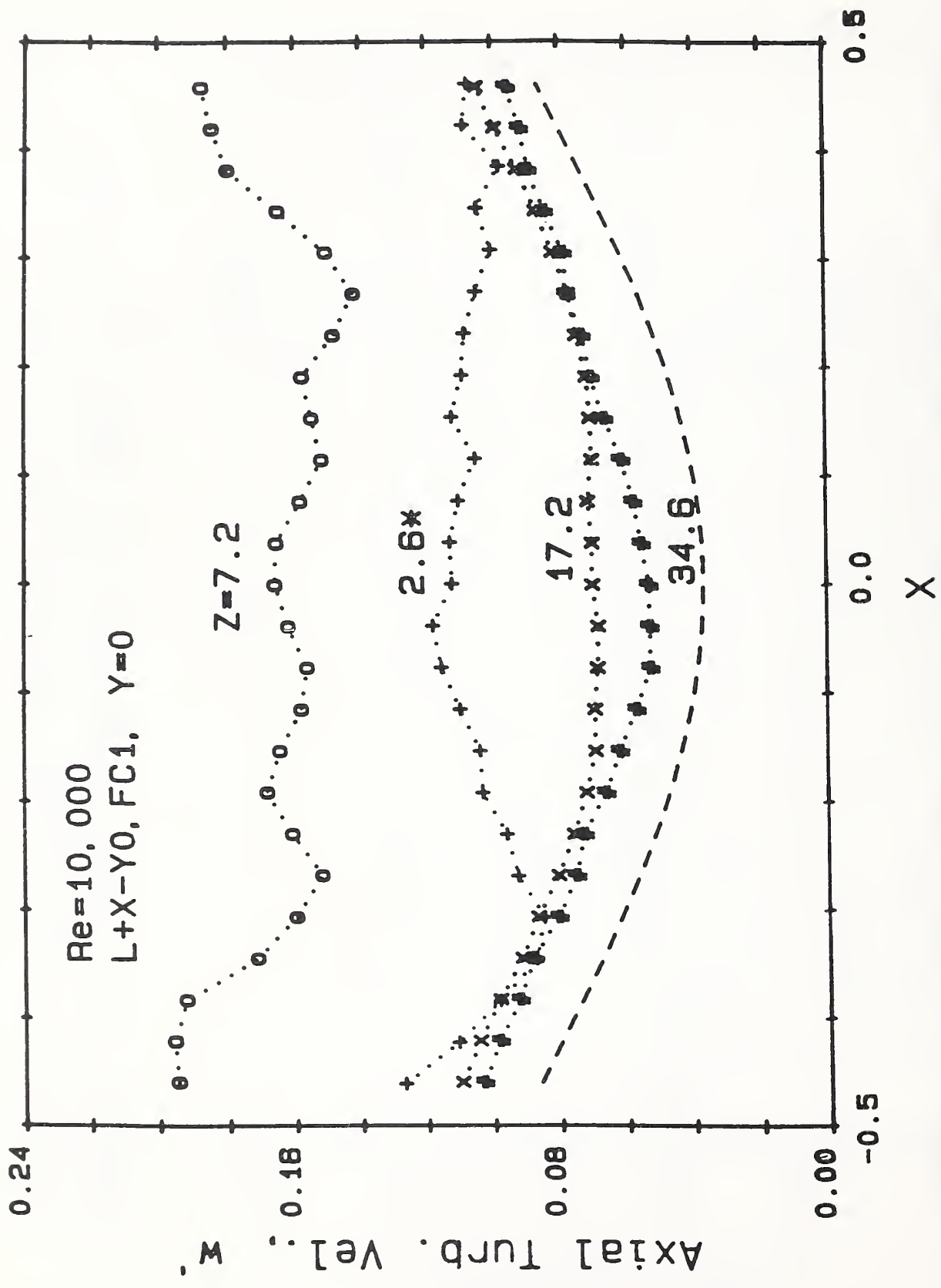


Figure 26. Profiles of the Axial Component of the Turbulent Velocity vs. Horizontal Radial Position at Different Downstream Locations for the Double Elbows-Out-Of-Plane and Tube Bundle Arrangement for $Re = 10K$.

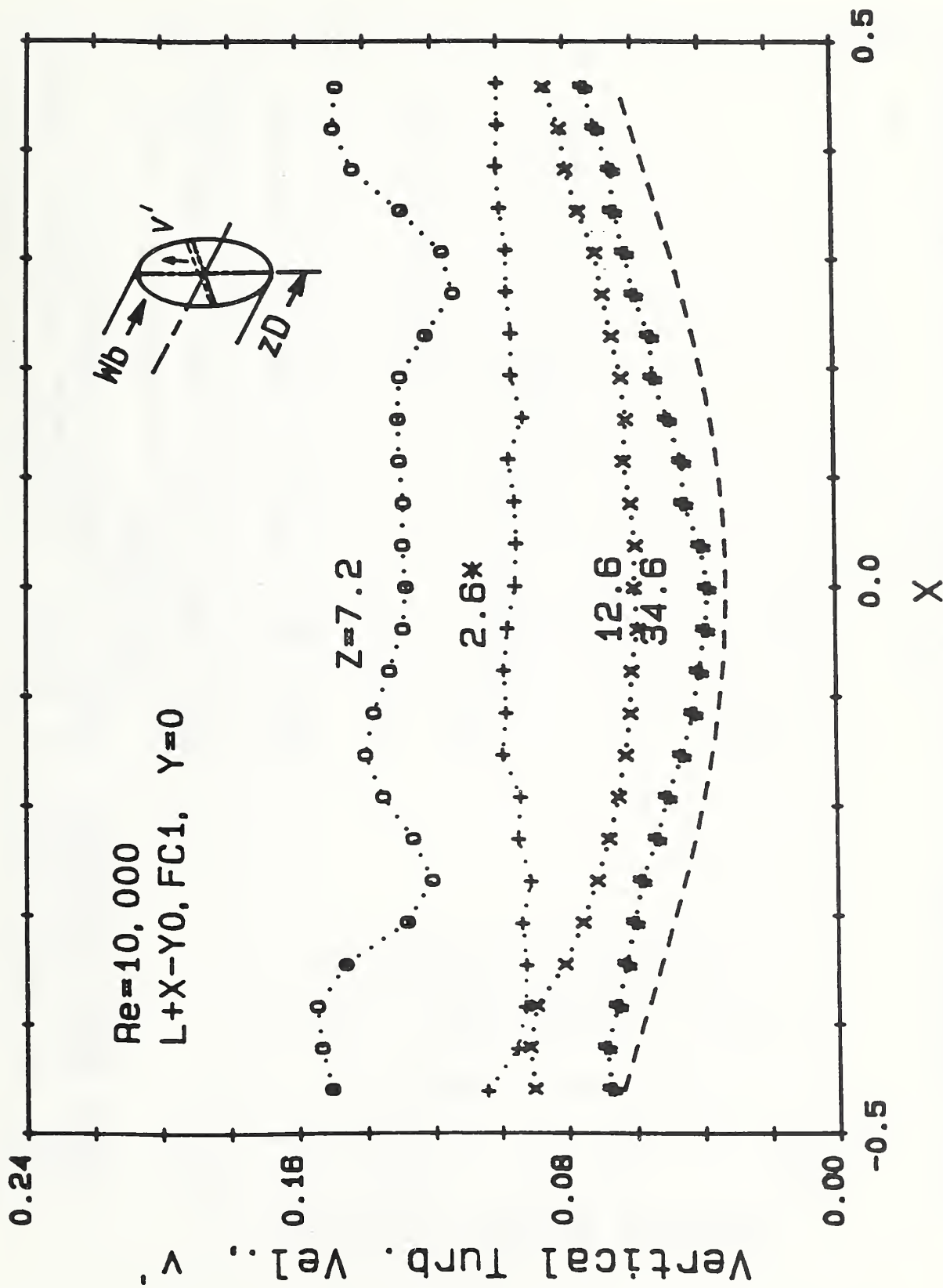


Figure 27. Profiles of the Vertical Component of the Turbulent Velocity vs. Horizontal Radial Position at Different Downstream Locations for the Double Elbows-Out-Of-Plane and Tube Bundle Arrangement for $Re = 10K$.

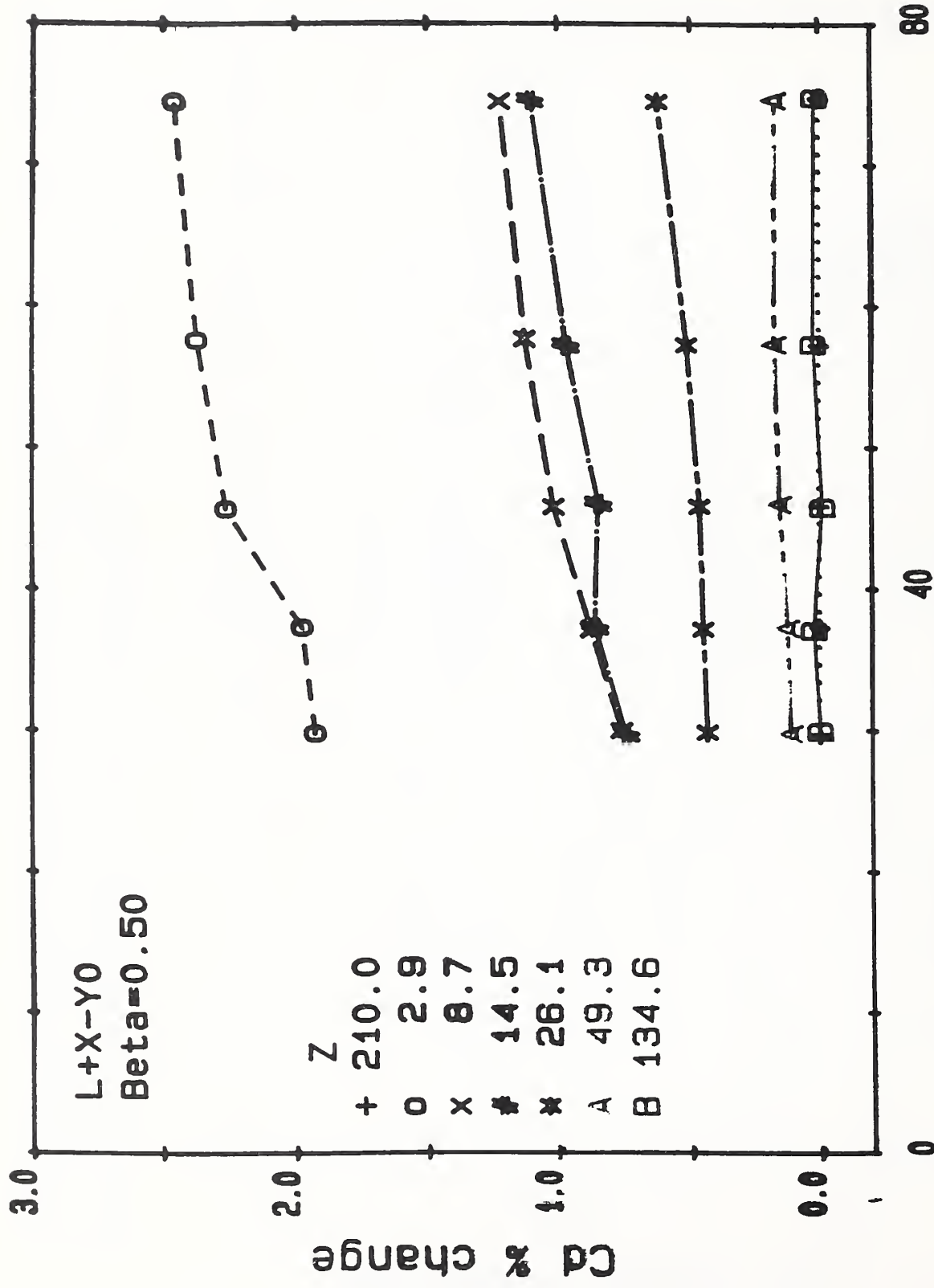


Figure 28(a). Percentage Change in Discharge Coefficient for a Beta = 0.5 Orifice Meter at Different Downstream Installation Positions from the Closely Coupled Double Elbows-Out-Of-Plane Configuration.

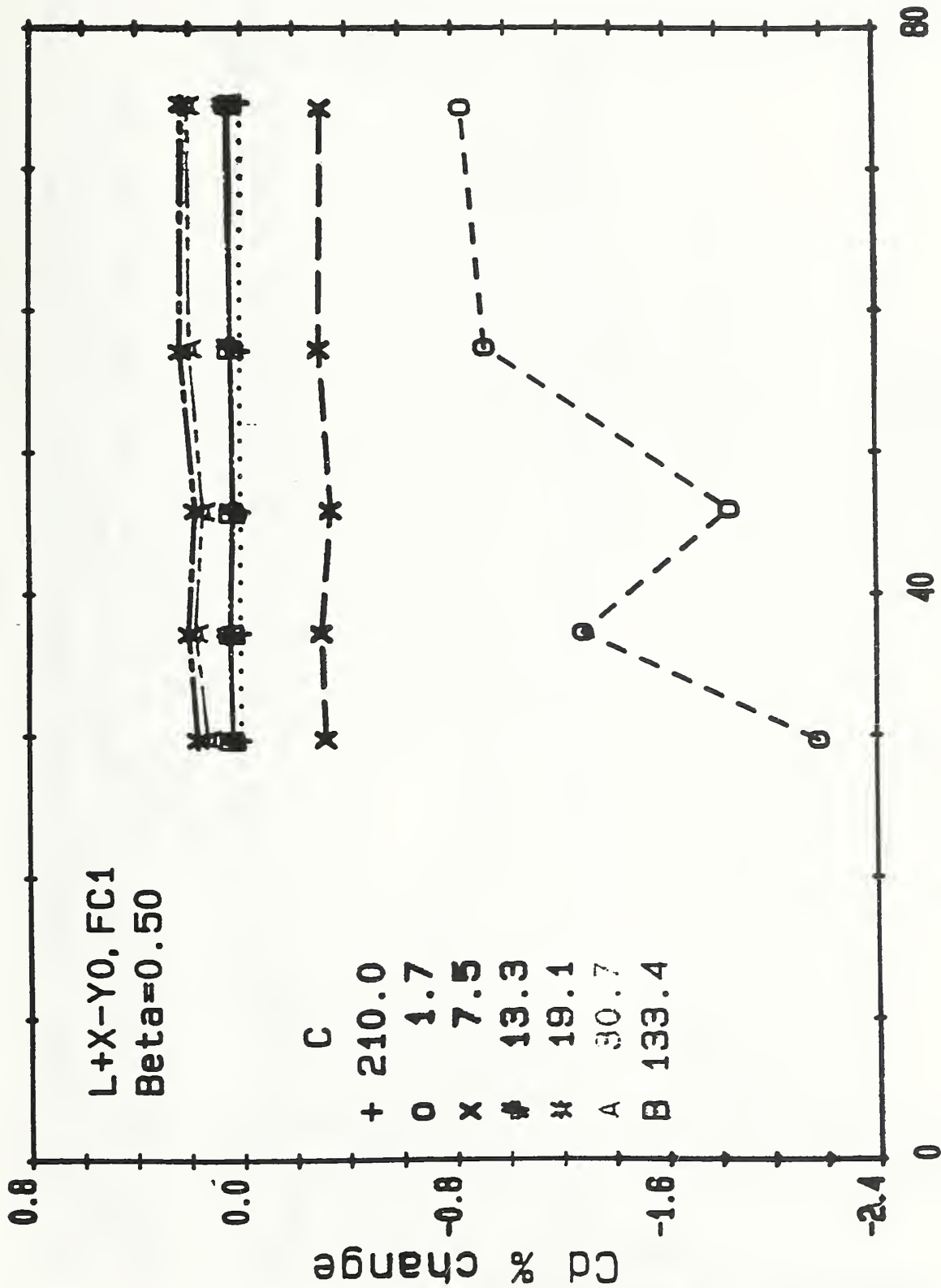


Figure 28(b). Percentage Change of the Mean Discharge Coefficient for a Range of Orifice Meters at Different Downstream Installation Positions from the Closely Coupled Double Elbows-Out-of-Plane and Tube Bundle Arrangement.

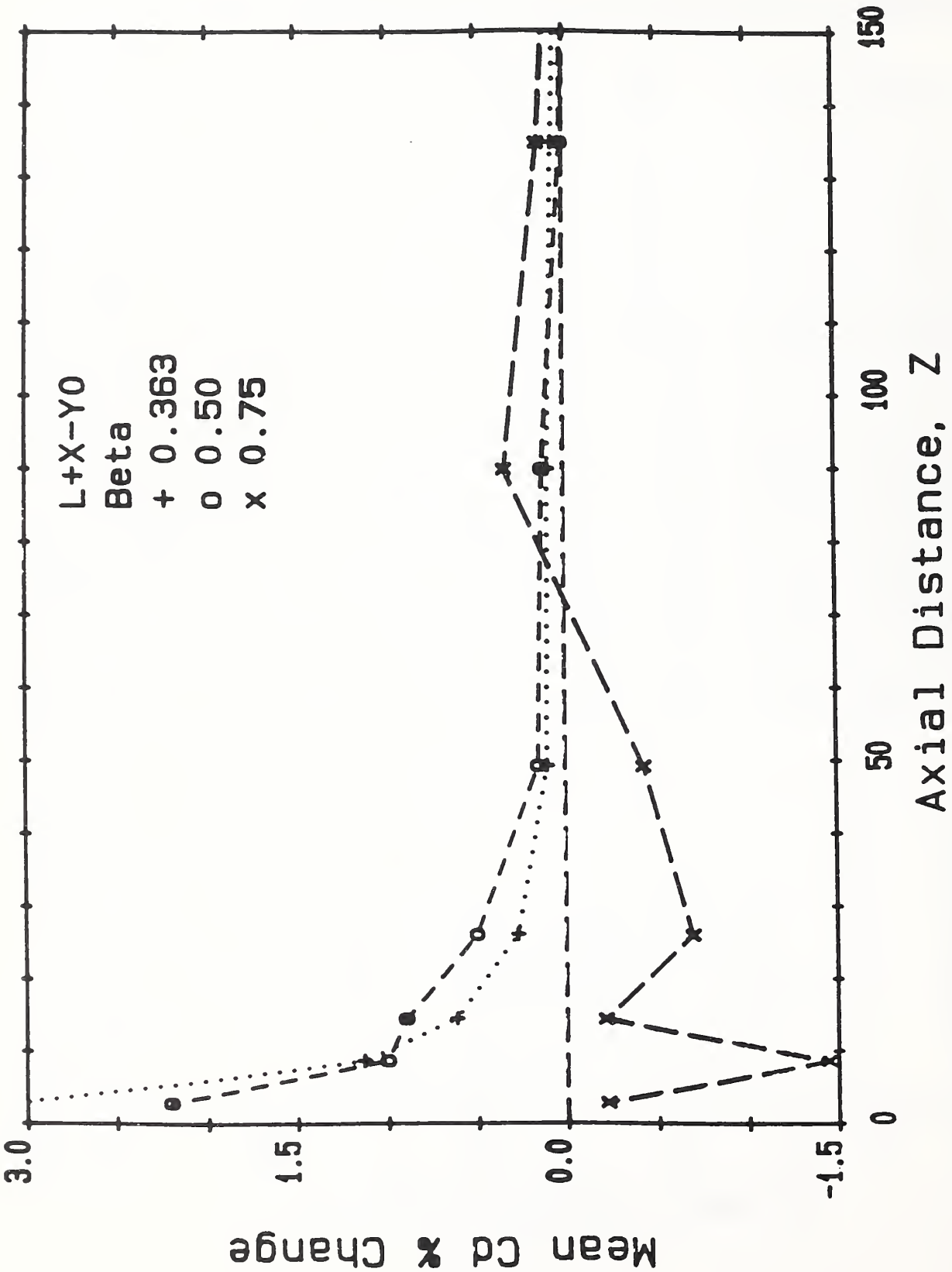


Figure 29(a). Percentage Change of the Mean Discharge Coefficient for a Range of Orifice Meters at Different Downstream Installation Positions from the Closely Coupled Double Elbows-Out-Of-Plane Configuration.

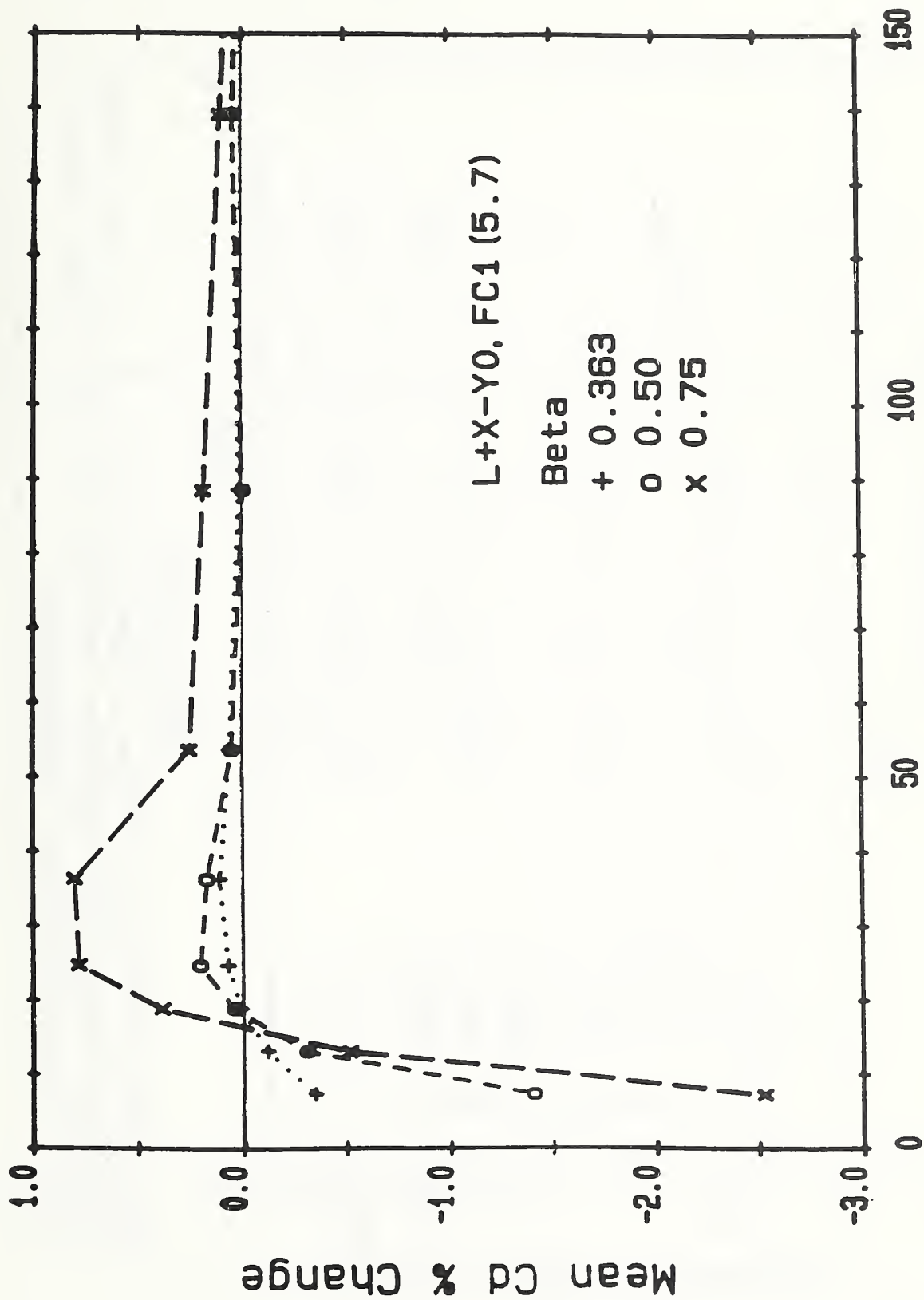


Figure 29(b). Percentage Change of the Mean Discharge Coefficient for a Range of Orifice Meters at Different Downstream Installation Positions from the Closely Coupled Double Elbows-Out-Of-Plane and Tube Bundle Arrangement.

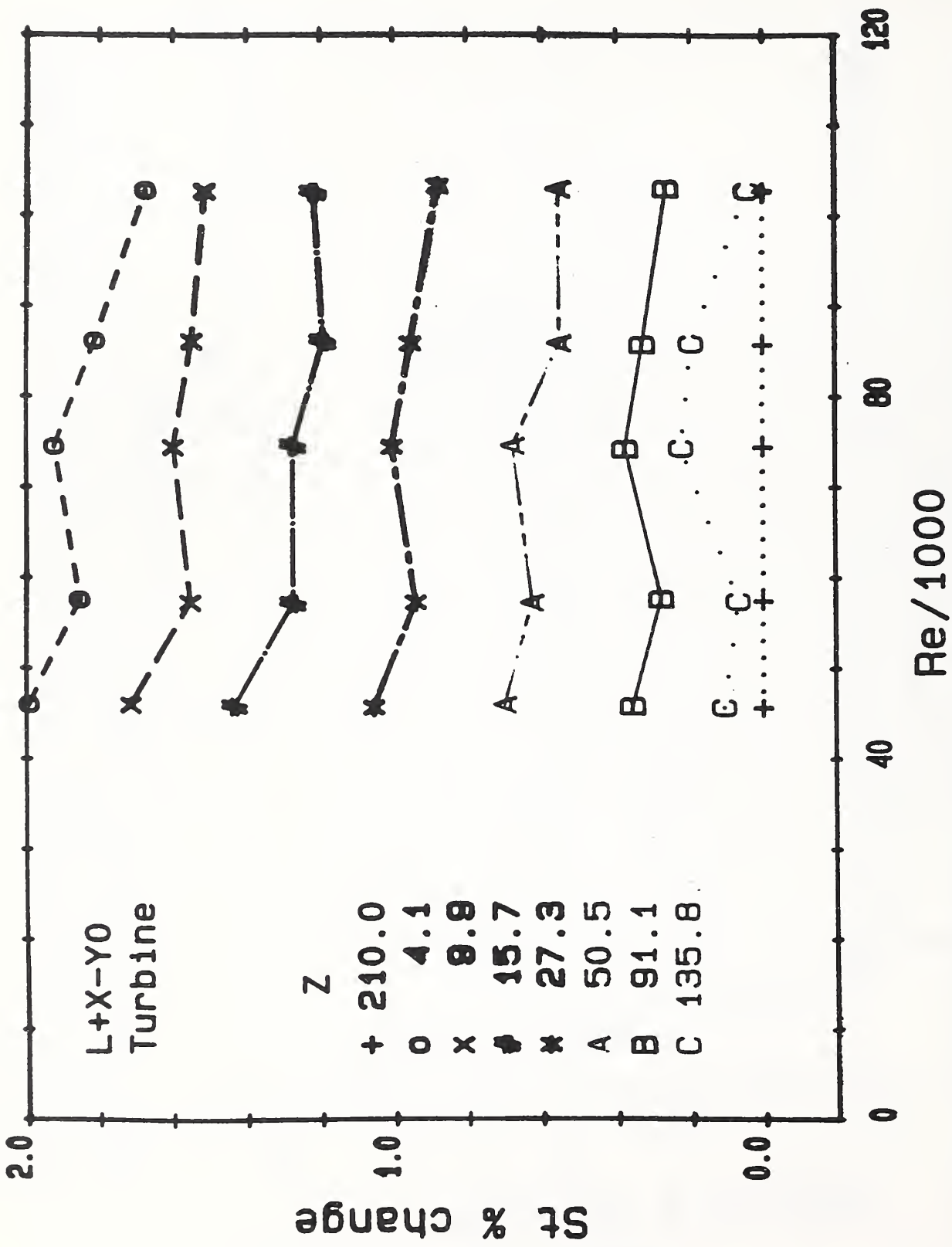


Figure 30(a). Percentage Change in Strouhal Number for a Turbine Meter at Different Downstream Installation Positions from the Closely-Coupled Double Elbows-Out-Of-Plane Configurations.

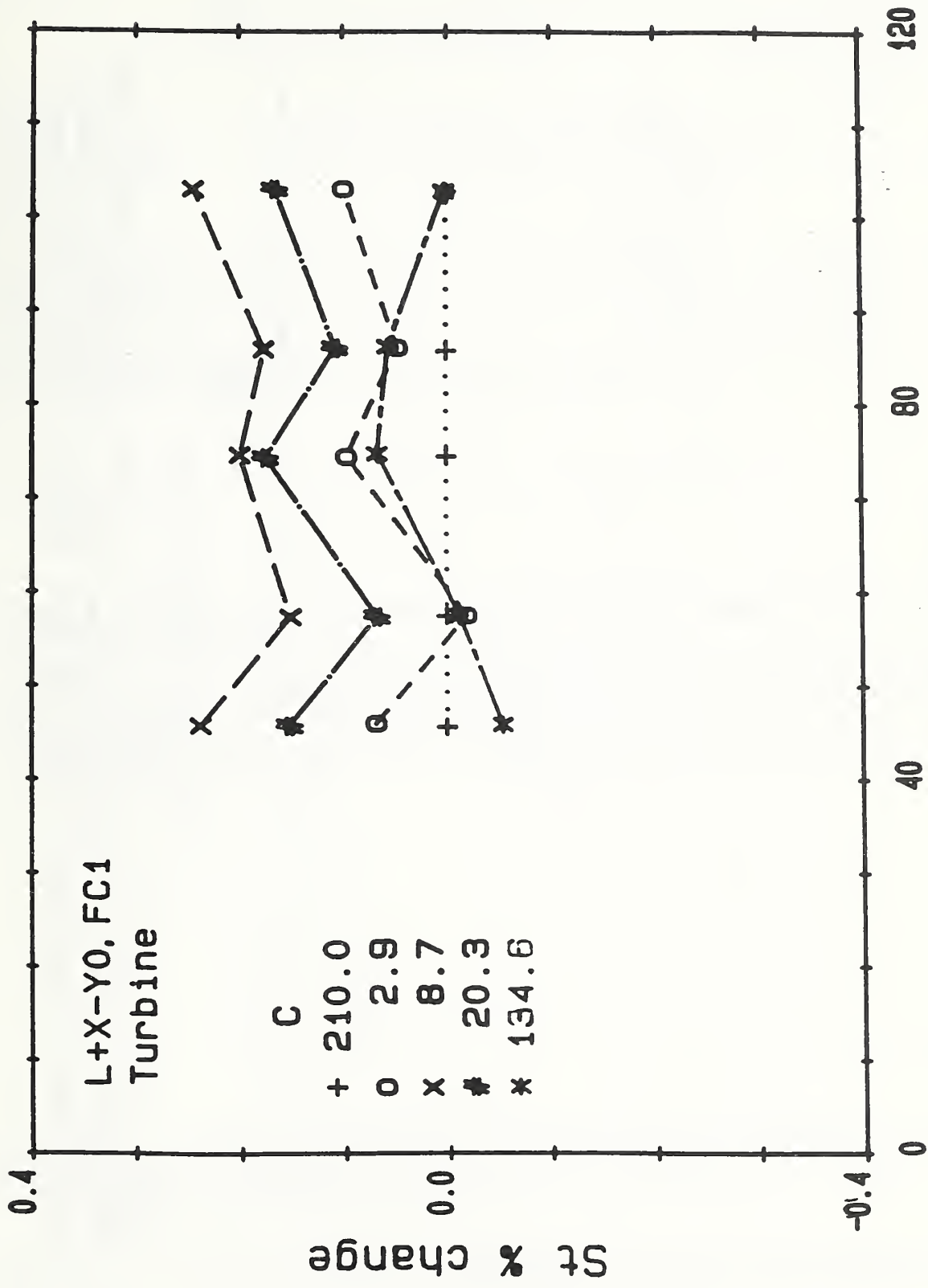


Figure 30(b). Percentage Change in Strouhal Number for a Turbine Meter at Different Downstream Installation Positions from the Closey Coupled Double Elbows-Out-Of-Plane and Tube Bundle Arrangement.

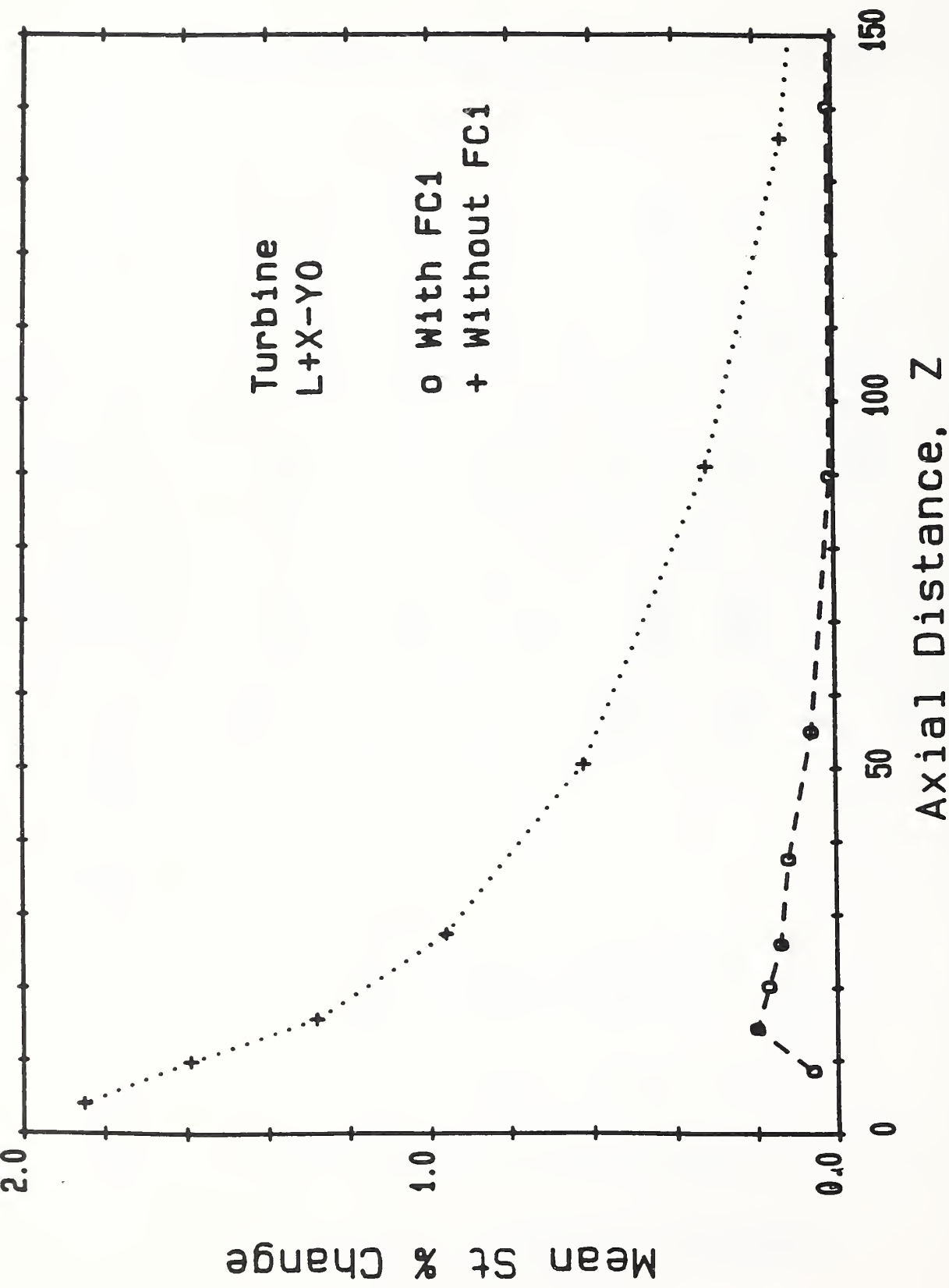


Figure 30(c). Percentage Change of the Mean Strouhal Number vs. Downstream Installation Position from the Closely Coupled Double Elbows-Out-Of-Plane Configuration With (o) and Without (+) the Tube Bundle.

NIST-114A
(REV. 3-90)

U.S. DEPARTMENT OF COMMERCE
NATIONAL INSTITUTE OF STANDARDS AND TECHNOLOGY

BIBLIOGRAPHIC DATA SHEET

1. PUBLICATION OR REPORT NUMBER

NISTIR 4751

2. PERFORMING ORGANIZATION REPORT NUMBER

3. PUBLICATION DATE

DECEMBER 1991

4. TITLE AND SUBTITLE

Summary Report of NIST's Industry-Government Consortium Research Program on Flowmeter Installation Effects with Emphasis on the Research Period May 1989 - February 1990: Tube Bundle Effects

5. AUTHOR(S)

G. E. Mattingly and T. T. Yeh

6. PERFORMING ORGANIZATION (IF JOINT OR OTHER THAN NIST, SEE INSTRUCTIONS)

U.S. DEPARTMENT OF COMMERCE
NATIONAL INSTITUTE OF STANDARDS AND TECHNOLOGY
GAITHERSBURG, MD 20899

7. CONTRACT/GRANT NUMBER

8. TYPE OF REPORT AND PERIOD COVERED

9. SPONSORING ORGANIZATION NAME AND COMPLETE ADDRESS (STREET, CITY, STATE, ZIP)

NIST Industry Consortium

10. SUPPLEMENTARY NOTES

11. ABSTRACT (A 200-WORD OR LESS FACTUAL SUMMARY OF MOST SIGNIFICANT INFORMATION. IF DOCUMENT INCLUDES A SIGNIFICANT BIBLIOGRAPHY OR LITERATURE SURVEY, MENTION IT HERE.)

This report presents results produced in a consortium-sponsored research program on flowmeter installation effects. This project is a collaborative one that has been underway for four years; it is supported by an industry-government consortium that meets twice yearly to review and discuss results and to plan subsequent phases of the work. This report contains the results and conclusions of the recent meeting of this consortium at NIST-Gaithersburg, MD in February 1990.

12. KEY WORDS (6 TO 12 ENTRIES; ALPHABETICAL ORDER; CAPITALIZE ONLY PROPER NAMES; AND SEPARATE KEY WORDS BY SEMICOLONS)

disturbed velocity profiles; flow conditioning; non-ideal flowmeter performance; swirl angle; swirl decay; swirled pipeflow; tube bundle

13. AVAILABILITY

UNLIMITED
 FOR OFFICIAL DISTRIBUTION. DO NOT RELEASE TO NATIONAL TECHNICAL INFORMATION SERVICE (NTIS).
 ORDER FROM SUPERINTENDENT OF DOCUMENTS, U.S. GOVERNMENT PRINTING OFFICE,
WASHINGTON, DC 20402.
 ORDER FROM NATIONAL TECHNICAL INFORMATION SERVICE (NTIS), SPRINGFIELD, VA 22161.

14. NUMBER OF PRINTED PAGES

47

15. PRICE

A03

